Detrital rutile geochemistry and thermometry as guides to provenance of Jurassic-Paleocene sandstones of the Norwegian Sea

Andrew Morton[1,2] and Simon Chenery[3]

[1] HM Research Associates, 2 Clive Road, Balsall Common, West Midlands CV7 7DW, UK

[2] CASP, University of Cambridge, 181a Huntingdon Road, Cambridge CB3 0DH, UK

[3] British Geological Survey, Keyworth, Nottingham NG12 5GG, UK

ABSTRACT

This paper explores the potential for use of rutile geochemistry as a provenance tracer in Jurassic-Paleocene sandstones in hydrocarbon exploration wells from the Norwegian Sea. Previous studies in this area, concentrating on provenance-sensitive heavy-mineral ratios, garnet geochemistry, tourmaline geochemistry, and detrital zircon geochronology, established the presence of five distinct sand types (MN1, MN2a, MN3, MN4, and MN5), sourced from different parts of the Norwegian and Greenland landmasses to the east and west of the basin. Approximately 50 rutile grains from two samples of each of these sand types have been analyzed by laser ablation inductively coupled plasma mass spectrometry. Differences in Cr and Nb contents indicate that there are significant variations in the relative abundance of rutiles derived from metamafic and metapelitic sources, with Norwegian-sourced sandstones (MN1, MN3 and MN5) having higher proportions of metamafic rutile compared with Greenland-sourced sandstones (MN2a and MN4).

Application of single-grain Zr-in-rutile geothermometry illustrates variations in metamorphic grade of the rutile sources. MN1 and MN5 rutiles were mainly derived from lower amphibolite- or eclogite-facies metapelitic rocks of the Caledonian Nappe Domain of mid-Norway, whereas MN3 rutiles were largely sourced from amphibolite- or eclogite-facies rocks of the Western Gneiss Region and adjacent parts of the Caledonian Nappe Domain, where metamafic gneisses and eclogites are widespread. Upper-amphibolite-facies metapelitic rocks, probably the Nathorst Land Group of East Greenland, were largely responsible for MN2a rutile assemblages. MN4 rutiles were mainly derived from granulite-facies metapelitic rocks, probably the Krummedal sequence of East Greenland.

The development of rutile geochemistry as a provenance tracer is especially important given the stability of rutile in both diagenetic and surficial weathering conditions. The technique yields information that can be utilised to reveal the ultimate source-rock lithology and metamorphic facies, even in highly modified sandstones that may have lost most other provenance information.

Keywords: rutile, provenance, Jurassic, Cretaceous, Paleocene, Norwegian Sea

INTRODUCTION

Heavy-mineral provenance studies are becoming progressively more sophisticated because an increasing number of detrital species are yielding provenance-sensitive mineral-chemical information (Mange and Morton 2007). Single-grain mineral-chemical studies initially focussed on amphibole (Mange-Rajetzky and Oberhänsli 1982), clinopyroxene (Cawood 1983), garnet (Morton 1985), tourmaline (Henry and Guidotti 1985), and chrome spinel (Pober and Faupl 1988), all of which show variations in major-element composition that can be readily determined by electron microprobe analysis. Several other minerals (notably epidote, staurolite, chloritoid, and titanite) also show variations in major-element compositions, but their potential application in provenance studies has not been fully explored, despite the work of, among others, Asiedu et al. (2000), Lonergan and Mange-Rajetzky (1994), Morton (1991), and Spiegel et al. (2002). A third group of detrital heavy minerals (notably apatite and zircon) show relatively limited variations in major-element compositions but display trace-element variations that have demonstrable value in provenance studies (Owen 1987; Belousova et al. 2002a, 2002b; Morton and Yaxley 2007).

An exciting recent development in mineral-chemical provenance studies concerns advances in understanding of the geochemistry of rutile. Rutile (TiO_2) predominantly forms in medium- to high-grade (greenschist- to granulite-facies) metamorphic rocks, and although it has been recorded in plutonic rocks, such as granitoids and anorthosites (Deer et al. 1992), it is scarce or absent in most igneous and low-grade metamorphic rocks (Force 1980, 1991). The lack of variation in major-element composition has, until recently, precluded the application of rutile geochemistry in provenance studies. For example, Preston et al. (1998) and Preston et al. (2002) demonstrated that detrital rutile in Triassic continental red-beds in

the Beryl Field, North Sea, comprises almost pure TiO_2, with only a small proportion containing appreciable Nb_2O_5 or FeO.

The recognition that a large number of trace elements (V, Cr, Fe, Al, Nb, Sn, Sb, Ta, W, Zr, Mo, Hf, Th, and U) may substitute for Ti in the rutile lattice led Zack et al. (2002), Zack et al. (2004a), and Zack et al. (2004b) to undertake electron microprobe and laser ablation inductively coupled plasma mass spectrometry (LA-ICP-MS) analyses on rutile to test if trace-element signatures could be used as a provenance tracer. This work had two significant conclusions. Firstly, they showed that the two principal rutile hosts (metapelitic and metamafic rocks) can be distinguished on the basis of Nb and Cr contents in rutile. Secondly, they showed that the Zr content of metapelitic rutile is dependent on temperature of formation, indicating that Zr in rutile can be used to measure maximum metamorphic temperatures. This single-grain Zr-in-rutile geothermometer was the first of its kind to be used in provenance studies.

Subsequent applications of detrital rutile geochemistry by Stendal et al. (2006), Triebold et al. (2007), and Meinhold et al. (2008) have demonstrated the effectiveness of the method in identifying sources and constraining the metamorphic evolution of the hinterland. Meinhold et al. (2008) suggest that the Zr-in-rutile geothermometer may be applicable not only to metapelitic rutiles but also to those of metamafic origin. Triebold et al. (2007) showed that high-grade metamorphic rutile survives metamorphic conditions on a retrograde path below 550°C, thereby preserving its chemical signature to much lower temperatures, and Stendal et al. (2006) showed that rutile does not always break down during low-grade (greenschist-facies) metamorphism, as was previously thought (Force 1980; Zack et al. 2004b).

The recognition that mineral-chemical analysis of detrital rutile may yield significant provenance information is of particular importance because of the stability of rutile under both burial diagenetic and surficial weathering conditions (Hubert 1962; Morton and Hallsworth 1999, 2007). The ultrastable nature of rutile means that crucial provenance information can be gathered from highly modified heavy-mineral assemblages that may have lost considerable amounts of provenance information. The stability of rutile, however, means that it is commonly present as a recycled phase, and thus geochemical analysis of this phase provides information on the composition and metamorphic grade of the ultimate source rocks. In the case of recycled sediment, the technique could be used to evaluate recycling pathways, by comparing rutile compositions in potential parent sandstones with those found in the daughter sediment.

Previous papers investigating sediment provenance using rutile geochemistry (Zack et al. 2004b; Stendal et al. 2006; Triebold et al. 2007; Meinhold et al. 2008) have been undertaken effectively in isolation, without additional provenance information except, in some cases, basic heavy-mineral analysis and whole-rock geochemistry. Consequently, it is not known whether rutile geochemical data are more or less effective at differentiating and constraining provenance compared with other techniques. The purpose of this paper is to assess the sensitivity of rutile geochemistry as a provenance tool, by analysing sandstones known to be derived from different sources on the basis of other, more well-established provenance techniques. This case study deals with Jurassic, Cretaceous, and Paleocene sandstones from the Norwegian Sea (Fig. 1), which have already been extensively studied using a combination of provenance-sensitive heavy mineral ratios, garnet geochemistry, tourmaline geochemistry, and detrital zircon geochronology (Fonneland et al. 2004; Morton et al. 2005a; Morton et al. 2005b; Morton et al. 2009). Additional objectives of the study were to provide additional

constraints on composition and metamorphic grade of the ultimate source regions and to assess the value of rutile geochemistry in the more deeply-buried parts of the basin where some key provenance indicator minerals (notably garnet) are absent due to diagenetic modification (Walderhaug and Porten 2007). The results of the study show that rutile geochemical data are entirely consistent with the existing heavy mineral evidence, and clearly establish the value of this technique for provenance studies.

JURASSIC-PALEOCENE SAND PROVENANCE IN THE NORWEGIAN SEA

The sedimentary basins of the Norwegian Sea (Fig. 1) formed as a result of multiple rift events through the late Paleozoic to the Paleogene, prior to the opening of the northern North Atlantic in the Paleogene. Evidence for rifting in the Carboniferous and the Early Triassic comes from East Greenland to the west (Stemmerik et al. 1993; Surlyk 1990; Seidler et al. 2004), with mid-Jurassic events recognized both in East Greenland (Price and Whitham 1997) and the Halten Terrace area (Corfield et al. 2001). Intense Late Jurassic-Early Cretaceous rifting is well documented across the rift in East Greenland (Surlyk 1990) and Mid Norway (Swiecicki et al. 1998; Doré et al. 1999), leading to the formation of the Vøring and Møre basins (Brekke et al. 1999), both of which contain very thick Cretaceous successions. A subsequent Late Cretaceous (Turonian) rift event affected the Vøring Basin, but apparently not the Møre Basin (Brekke et al. 1999). The final rift phase affecting the region was the Paleocene-Eocene rifting associated with continental breakup (Doré et al. 1999).

The Jurassic succession in the Norwegian Sea is known only from the Halten Terrace and adjacent areas close to the Norwegian landmass (Fig. 1), since it is deeply buried farther west

in the Vøring and Møre basins, and has therefore not been penetrated by hydrocarbon exploration wells. Sandstones are present in the Lower-Middle Jurassic Åre, Tilje, Ror, Ile, Not, and Garn formations (Dalland et al. 1988) but become scarce in the Late Jurassic, which is dominated by deposition of organic-rich mudrocks. The Åre Formation (latest Triassic to Early Pliensbachian) was deposited in a fluvial to deltaic setting (Dalland et al. 1988; Kjaerefjord 1999; Svela 2001). The overlying Tilje Formation (Sinemurian to Pliensbachian) is composed of interbedded sandstones, mudstones, and siltstones, deposited in a deltaic to shallow marine setting (Dalland et al. 1988; Martinius et al. 2001; Svela 2001). The Ror Formation (Toarcian) consists of marine shelf deposits comprising sandy mudstones with coarsening-upwards sandier units (Dalland et al. 1988). The Ile Formation (Aalenian) consists of a coarsening-upwards sandstone-dominated unit deposited on an initially tidally dominated and subsequently wave dominated marine shelf, and includes tidal-channel and subtidal-flat deposits deposited by a tidally influenced delta (Harris 1989; McIlroy 2004; Martinius et al. 2005). The Not Formation (Aalenian) was deposited on a marine shelf and comprises heavily bioturbated mudstones coarsening up into sandy mudstones (Harris 1989). The Garn Formation (Aalenian-Bajocian) consists of coarse-grained sandstones deposited in fluvial, delta-top and shallow marine settings (Dalland et al. 1988). The Garn Formation is overlain by the Bajocian-Oxfordian mudstone-dominated Melke Formation, deposited in an offshore shelf setting, and the Oxfordian-Ryazanian Spekk Formation, dominated by organic-rich marine mudstones (Dalland et al. 1988).

Cretaceous-Paleocene sandstones tend to occur in the deeper-water areas of the Norwegian Sea, in the Vøring and Møre basins (Fig. 1). They range in age from Albian to Paleocene and are ascribed to the Lange, Lysing, Kvitnos, Nise, Springar, and Tang Formations (Dalland et al. 1988; Vergara et al. 2001). They were deposited in deep-water slope and submarine fan

environments (Shanmugam et al. 1994; Morton and Grant 1998; Kittilsen et al. 1999; Gjelberg et al. 2001).

Five different sand types (termed MN1, MN2, MN3, MN4, and MN5) have been identified in the Jurassic-Paleocene of the Norwegian Sea on the basis of variations in the provenance-sensitive heavy-mineral ratios apatite:tourmaline (ATi), garnet:zircon (GZi), rutile:zircon (RuZi), monazite:zircon (MZi) and chrome spinel:zircon (CZi), garnet geochemistry, tourmaline geochemistry, and detrital zircon geochronology (Morton et al., 2005a, 2005b, 2009). These five sand types are interpreted as being derived from different source areas that lay to the east (Scandinavia) and west (Greenland) of the Norwegian Sea (Fig. 1). As far as is possible, the characteristics of the five sand types are illustrated with data from the samples used in the rutile geochemical study. In cases where mineral-chemical data are not available from these specific samples, samples with comparable provenance-sensitive ratio data from adjacent depths or from stratigraphically equivalent units in adjacent wells have been used.

MN1 Sand Type

MN1 sandstones (Fig. 2) have relatively high RuZi (> 35), relatively low ATi (< 20), low CZi (< 2), and low-moderate MZi (0-10). GZi is generally high (70-80) but is markedly reduced where burial-related garnet dissolution has taken place. MN1 garnet assemblages are rich in low-Mg, high-Fe+Mn, variable Ca types (Type B in the terminology of Morton et al. 2004 and Mange and Morton 2007) and correspondingly scarce in Type A (high-Mg, low-Ca) and Type C (high-Ca, high-Mg) garnets (Figs. 3 and 4). Tourmaline populations in MN1 sandstones (Figs. 5 and 6) have approximate equal numbers of Al-poor metasedimentary grains (Type E, as defined by Henry and Guidotti 1985) and Al-rich metasedimentary grains

(Type D), with minor types B and F. MN1 detrital zircon age spectra have one main peak at ~ 1780-1790 Ma, have minor representation of younger Proterozoic and Early Paleozoic ages, and lack Archean grains (Fig. 7). Sandstones with MN1 characteristics are found in Cretaceous-Paleocene successions bordering the Trondelag Platform, and were sourced from the Nordland area of the Scandinavian landmass, an area that comprises metasedimentary rocks of the Caledonian Nappe Domain and basement windows that expose the westerly extension of the Fennoscandian Shield (Skår 2002).

MN2 Sand Type

MN2 sandstones (Fig. 2) have lower RuZi than MN1 (mostly < 35), in conjunction with CZi of 1-7, MZi < 5, and GZi ~ 80 (except where burial-related garnet dissolution has taken place). ATi is mostly < 20, but in one well (6704/12-1, located on the Gjallar Ridge) values are significantly higher, up to 50. On the basis of differences in ATi, the MN2 group has been subdivided into two subgroups, MN2a and MN2b (Morton et al. 2005a). However, since rutiles have not been analyzed from the MN2b sand type, this subgroup is not discussed further here. MN2a garnet assemblages are similar to those of MN1, being rich in Type B and scarce in Types A and C (Figs. 3 and 4). However, the two sand types have distinctly different tourmaline assemblages, MN2a tourmaline populations having higher contents of the Al-rich metasedimentary (Type D) component (Figs. 5 and 6). MN2a zircon age spectra are considerably more complex than those of MN1, and include Archean, Paleoproterozoic, Mesoproterozoic, Early Paleozoic, Permian-Triassic, and mid-Cretaceous elements (Fig. 7). MN2a sandstones tend to occur in wells farther west compared with MN1, and are interpreted to be sourced from NE Greenland, with contributions from metasediments and granites of the

Caledonian fold belt, Archaean-Proterozoic crystalline basement rocks, possibly recycled from Paleozoic-Mesozoic clastic successions (Fig. 1).

MN3 Sand Type

MN3 sandstones (Fig. 2) have relatively low RuZi (< 40), low MZi (< 5), very low CZi (<1), high GZi (except where burial-related garnet dissolution has taken place), and relatively high ATi values (30-80). Garnet assemblages are distinctive, being rich in the Type C (high-Mg, high-Ca) component (Figs. 3 and 4). Tourmaline assemblages are also distinct from those in MN1 and MN2a, with Al-poor metasedimentary grains (Types E and F) being more abundant than Al-rich metasedimentary (Type D) grains (Figs. 5 and 6). The detrital zircon age spectrum comprises one main group that peaks at ~ 1660 Ma with a subordinate group between ~ 900 Ma and ~ 1100 Ma (Fig. 7). MN3 sandstones are present in wells along the Norwegian margin of the Møre Basin (Fig. 1), and are interpreted to be sourced from western Norway, including the Western Gneiss Region, an area where high-grade metamafic rocks and eclogites are widespread.

MN4 Sand Type

The most distinctive feature of sand type MN4 is the high abundance of Type A garnet (Figs. 3 and 4), which contrasts with sand types MN1 and MN2, both of which are rich in Type B, and to sand type MN3, which is rich in Type C. MN4 sandstones also have extremely high RuZi values (> 60), considerably greater than MN2 and MN3 sandstones, and greater than the majority of MN1 sandstones (Fig. 2). MN4 sandstones have higher MZi values than MN2, MN3 and the majority of MN1 sandstones (Fig. 2). By contrast, CZi values are extremely low

(< 1). Tourmaline populations (Figs. 5 and 6) are similar to those found in sand type MN2a, being dominated by the Al-rich metasedimentary component (Type D). Zircon age spectra (Fig. 7) contain a wide range of components, with the Archean, Paleoproterozoic, Mesoproterozoic, and Early Paleozoic all represented. In broad terms, the MN4 zircon age spectra are comparable to those of MN2, but they differ in detail, particularly regarding the abundance of Early Paleozoic zircons, which are more common in MN4 compared with MN2 (Fig. 7). The source of the MN4 sand type is interpreted to lie in central East Greenland (Fig. 1), on account of the zircon age data, the presence of similar MN4 sandstones in the Cretaceous of the Kangerlussuaq area (Whitham et al. 2004), and on the occurrence of moraine in East Greenland with similar characteristics (Morton et al. 2009).

MN5 Sand Type

Sand type MN5 is a relatively heterogeneous group, with a wider range of provenance-sensitive ratios than the other sand types identified in the Norwegian Sea (Fig. 2). RuZi values are mostly in the 40-60 range (Fig. 2), indicating greater affinity with MN1 than with MN2, MN3, or MN4. ATi values show a wide range but are generally higher than in MN1, MN2, and MN4. CZi values are variable; some MN5 sandstones have much higher CZi than any of the other sand types (Fig. 2), but CZi can also be relatively low (~ 1-3). As with all of the other sand types in the area, GZi values were originally high but now show a wide range due to variable degrees of garnet dissolution. Garnet assemblages are low in Type A, the main component being Type B with significant subsidiary amounts of Type C (Figs. 3 and 4). The higher proportion of Type C garnets distinguishes MN5 from MN1 and MN2. Tourmaline populations (Figs. 5 and 6) tend to be relatively rich in Type F, although to a lesser degree than sand type MN3. The detrital zircon age spectrum lacks an Archean

component, and comprises Paleoproterozoic-Mesoproterozoic and early Paleozoic grains (Fig. 7), the most prominent peak being at ~ 1650 Ma. MN5 sandstones are interpreted as having been derived from Mid-Norway (Fig. 1), with contributions from metasediments and interleaved ophiolites of the Caledonian Nappe Domain, together with metamafic rocks similar to those of the Western Gneiss Region that supplied MN3.

DETRITAL RUTILE PROVENANCE IN THE NORWEGIAN SEA

Two samples from each of the sand types described above were selected for rutile geochemical analysis by LA-ICP-MS, following methods described in the Appendix. Rutile geochemical data are supplied as a Supplementary Publication. The samples were chosen to cover a wide range of burial depths, to assess the value of the technique compared with garnet geochemistry, which cannot be used in provenance studies of deeply buried sediments owing to diagenetic depletion of garnet (Fig. 8). Accordingly, GZi values are significantly lower in the deeper of each pair of samples, with the exceptions of samples from MN1 and MN4. In these cases, although there is surface textural evidence for advanced garnet dissolution in the deeper samples (in the form of large-scale etch facets as described by Turner and Morton 2007), GZi values are no lower in the deeper samples compared with those from shallow depths.

Zack et al. (2004b) were the first to propose that the two main sources of rutile (metapelites and metabasites) can be distinguished on the basis of Nb and Cr contents, with metapelitic rutiles having 900-2700 ppm Nb and < 1000 ppm Cr, and metamafic rutiles having a relatively wide range in Cr and generally low Nb. The criteria for discrimination of metapelitic and metamafic rutile proposed by Zack et al. (2004b) have been revised in

subsequent studies by Triebold et al. (2007) and Meinhold et al. (2008). Triebold et al. (2007) proposed that rutiles with Cr > Nb have a metamafic source whereas rutiles with Cr < Nb are of metapelitic origin. Meinhold et al. (2008) adopted this criterion except for rutiles with Nb < 800 ppm (close to the lower limit of metapelitic rutile as originally proposed by Zack et al, 2004b), all of which they classified as metamafic. In this paper, we follow the discrimination proposed by Meinhold et al. (2008). Cr-Nb plots of rutiles from the Norwegian Sea Jurassic-Paleocene demonstrate the existence of major differences in rutile provenance between sand types. For example, the majority of the 48 rutiles analyzed from the Agat Formation (Cretaceous) in well 35/3-5 (sand type MN3) are of metamafic origin (60% of the population); by contrast, 89% of the 54 rutiles analysed from the Garn Formation (Jurassic) in well 6406/2-1 (sand type MN4) were derived from metapelitic sources (Fig. 9).

Two alternative calculations have been proposed for the determination of formation temperature of rutile using Zr contents. The empirical Zr-in-rutile temperature calculation proposed by Zack et al. (2004a), based on data from rutile-, quartz-, and zircon-bearing metamorphic rocks formed at temperatures between 430°C and 1100°C, expresses temperature as

$$T\ (^{o}C) = 127.8 \times \ln(\text{Zr ppm}) - 10$$

with an error of ± 50°C.

Watson et al. (2006) presented an alternative thermometric calculation based largely on experimental data, with additional constraints provided by rutiles from metamorphic rocks, which expresses temperature as

$T\ (^{o}C) = 4470/(7.36 - \log_{10}[Zr\ ppm]) - 273$

with an error of ± 20°C.

The Zack et al. (2004a) and Watson et al. (2006) geothermometers (T_Z and T_W, as expressed by Meinhold et al. 2008) intersect at approximately 540°C, but show appreciable differences at both lower and higher temperatures, possibly indicating a degree of pressure dependence (Watson et al. 2006). These differences are demonstrated in Fig. 10, which compares T_Z and T_W for rutiles in well 6406/2-1 (sand type MN4). Both calculations show that the majority of rutiles in this sample formed under granulite-facies conditions, but T_Z (850-1050^{o}C) is considerably higher than T_W (750-900^{o}C). The Zack et al. (2004a) geothermometer therefore suggests that the MN4 source in central East Greenland includes widespread ultrahigh-temperature (UHT) granulite-facies metamorphic rocks, which are formed at temperatures over 900^{o}C (Harley 1998). Although migmatites and other sillimanite-bearing metamorphic rocks are common in central East Greenland (e.g., Dhuime et al. 2007), there are no reports of ultrahigh-temperature metamorphic rocks in this region (although the geology of inland Greenland is poorly known because of the vast ice sheet). On the basis of the known geological framework, therefore, it appears that the Watson et al. (2006) Zr-in-rutile geothermometer provides a more realistic estimate of high-grade rutile formation temperatures than the Zack et al. (2004a) geothermometer, a conclusion also reached by Meinhold et al. (2008). In the subsequent discussion, therefore, we refer only to the Zr-in-rutile geothermometer of Watson et al. (2006).

Rutile geochemical characteristics of the ten samples (Fig. 11) show the existence of major variations between the five different sand types in terms of both source composition and metamorphic temperature. By contrast, there are comparatively few differences between rutile populations in samples of the same sand type. These observations confirm that rutile geochemistry is a powerful tool for discriminating sand provenance and provides valuable support for the existing categorization of sand type achieved using provenance-sensitive heavy-mineral ratios, garnet and tourmaline geochemistry, and detrital-zircon geochronology. Moreover, the rutile data provide important additional constraints on the lithological nature and metamorphic history of the ultimate source areas.

MN1 Rutiles

The majority of the MN1 rutiles were derived from metapelitic sources (69-76%), compared with 24-31% from metamafic rocks, and most were formed under amphibolite- or eclogite-facies conditions, although many of the metamafic rutiles in the Tang Formation of well 6710/10-1 yield greenschist-facies temperatures. There is a distinct, though relatively subtle, difference in metamorphic temperatures between the two samples. The rutiles from the Tang Formation of well 6710/10-1 fall predominantly in the lower amphibolite-facies range (550-650^{o}C), whereas the Lange Fm sample from well 6507/2-3 contains a larger number of upper amphibolite-facies rutiles in the 650-700^{o}C bracket. There are significant differences in both age and geographical location for the two MN1 samples, and the observed difference in rutile metamorphic temperature could relate either to lateral variations in metamorphic grade in the MN1 source region or to temporal changes in drainage pattern.

Analysis of additional samples is needed in order to evaluate these possibilities, but the initial findings suggest that rutile geochemistry may provide added sophistication to the understanding of the provenance of the MN1 sandstones. The rutile data are compatible with ultimate derivation from the Nordland region of Norway, an area that contains the Upper and Uppermost allochthons of the Caledonian Nappe Domain, together with basement windows that expose the westerly extension of the Fennoscandian Shield (Skår 2002). The Upper Allochthon comprises ophiolites of oceanic origin, igneous rocks of magmatic-arc affinity, and marginal-basin successions within or peripheral to the Iapetus Ocean, whereas the Uppermost Allochthon consists largely of metasedimentary rocks (Roberts 2003). Metamorphism within the Upper and Uppermost allochthons generally took place under amphibolite- and eclogite-facies conditions, although higher-temperature (granulite-facies) conditions have been identified locally, such as in the Seve Nappes (Williams and Claesson 1987), located south of the Nordland region. The geological framework of the Nordland region therefore appears to be compatible with the compositions of the rutiles found in MN1 sandstones.

MN2a Rutiles

Rutile populations in the two MN2a sandstones from well 6706/11-1 contain only 4-13% of the metamafic component, significantly less than in MN1 (Fig. 11). The difference in rutile provenance is further emphasized by the temperature plots. The two MN2a sandstones have closely comparable temperature distributions, dominated by rutiles formed under upper amphibolite-facies (650-750^{o}C) conditions (Fig. 11). Rutile geochemistry therefore supports the evidence for a difference in provenance between MN1 and MN2a sandstones as

established by heavy-mineral ratios, garnet and tourmaline geochemistry, and detrital-zircon geochronology (Morton et al. 2005a).

The strong similarity in rutile compositions in the two MN2a samples is evident despite the marked difference in garnet abundance. GZi is high (77.8) in the sample from 2315.30 m depth but low (2.0) in the sample from 3749.90 m depth. The decrease in GZi in the more deeply buried sample is due to burial-related diagenetic dissolution of garnet (Morton and Hallsworth 2007; Walderhaug and Porten 2007). Hence, rutile geochemistry can be used to compare provenances of sandstones that have undergone different degrees of modification by diagenetic processes.

The MN2a sandstones are interpreted to be derived from NE Greenland, with a complex provenance including Archean and Early Proterozoic crystalline basement, metasediments of the Caledonian fold belt, Caledonian granites, and Permian-Triassic felsic igneous rocks. Given these components, the metasediments of the Caledonian fold belt are the most likely source of the rutile in the MN2a sandstones, although crystalline basement is also likely to have been involved, and recycling through one or more intermediate sedimentation phases is likely. The metasediments of the East Greenland Caledonian fold belt comprise the Krummedal sequence, overlain by the Eleanore Bay Supergroup (Escher and Pulvertaft 1995). Published data on metamorphic conditions in the metasedimentary successions range from high-grade in the Krummedal sequence, through upper amphibolite-facies (c. 650-700^{o}C) in the Nathorst Land Group (the lower part of the Eleanore Bay Supergroup), to weakly or unmetamorphosed in the uppermost parts of the sedimentary pile (Kalsbeek et al. 2000; Peucat et al. 1985; White et al. 2002; Dhuime et al. 2007). The Nathorst Land Group therefore appears to be the most likely ultimate source for the rutiles in the MN2a sandstones,

although (as indicated above) crystalline basement may also have been involved. Compared with Scandinavia, metamafic rocks are significantly less abundant in the Caledonian fold belt of East Greenland, compatible with the smaller numbers of metamafic rutiles present in the MN2a sandstones.

MN3 Rutiles

The rutile populations in the two MN3 sandstones (Fig. 11) are markedly different from those of the other sand types, being especially rich in the metamafic variety (forming 60-62% of the rutile assemblages). The predominance of metamafic rutiles is in accord with the abundance of Type C (high-Mg, high-Ca) garnets in MN3 sandstones (Figs. 3 and 4), which are typically derived from eclogites and granulite-facies metamafic rocks (Mange and Morton 2007). MN3 sandstones are interpreted to have been derived from western Norway, an area that includes the Western Gneiss Region and the Middle Allochthon of the Caledonian Nappe Domain (Morton et al. 2005a). Both of these regions are characterized by widespread high-grade mafic gneisses (including eclogites), locally with pyroxenites and peridotites (Qvale and Stigh 1985). The abundance of metamafic rutile is therefore in accord with the geological framework of the inferred source area.

The temperature plots of the two MN3 samples show distinct differences. Although both samples contain mainly amphibolite- or eclogite-facies rutiles, the sample from well 6305/8-1 has a distinctly bimodal character and includes a significant proportion of granulite-facies grains. By contrast, calculated rutile temperatures in well 35/3-5 form a single broad peak with comparatively few granulite-facies grains. The difference in rutile temperature distributions between the two samples suggests that rutile geochemistry could prove useful in subdividing MN3 sandstones and might provide a greater resolution of provenance. It is

unclear on the basis of the available data whether the differences relate to geographic location or to age, since the two samples are from widely separated wells (Fig. 1) and different stratigraphic positions (Albian and Paleocene).

The bimodal temperature distribution shown by the rutiles in well 6305/8-1 is seen not only in the metapelitic component but also by the metamafic types (Fig. 11).The MN3 temperature plots therefore provide confirmation that temperature estimates can be reliably obtained from metamafic rutiles as well as from metapelitic rutiles, a feature also recognised by Meinhold et al. (2008).

MN4 Rutiles

The two MN4 rutile populations are readily distinguishable from those found in the other sand types on the basis of their formation temperatures (Fig. 11). Both samples have closely comparable temperature distributions: 82-89% of the rutiles have granulite-facies temperatures, peaking in the 800-850^{o}C bracket. Rutile formation temperatures in the two MN4 sandstone samples are therefore significantly higher than in any of the other sand types. The abundance of granulite-facies rutile is in accord with the evidence from the garnet geochemistry, since MN4 sandstones are characterized by Type A garnet assemblages, typically derived from high-grade granulite-facies metasedimentary rocks and charnockites (Sabeen et al. 2002; Mange and Morton 2007). Derivation from high-grade granulite-facies metasediments is therefore indicated, the most likely candidate being the Krummedal sequence in central East Greenland, which has undergone high-grade metamorphism and anatectic melting (Kalsbeek et al. 2000). In the two MN4 rutile populations, metapelitic types (76-89%) are significantly more abundant than metamafic types (11-24%). Metamafic rutiles

are therefore slightly more common in MN4 compared with MN2a (4-13%), also interpreted to be derived from East Greenland, but are less common than in MN1 (24-31%), MN3 (60-62%) and MN5 (24-33%), all of which are interpreted to have Norwegian sources.

MN5 Rutiles

Metapelitic types form 67-76% of the two MN5 rutile populations, indicating that although metapelites were the main source of rutile, metamafic rocks were also common in the hinterland. The temperature distributions of the two samples are closely comparable (Fig. 11). Both have predominantly amphibolite- or eclogite-facies temperatures peaking in the 550-650^{o}C (lower amphibolite) bracket, with a small number (10-22%) falling in the granulite-facies range. The MN5 rutile populations are similar to those of MN1, although MN5 has slight more metamafic rutile and granulite-facies rutile. Both MN1 and MN5 sandstones are interpreted as having been sourced from the Caledonian Nappe Domain of Scandinavia (Morton et al., 2005b; Morton et al., 2009), the MN1 source being located farther north and including exposures of Fennoscandian basement (Fig. 1). The similarity between the MN1 and MN5 rutile populations is consistent with this interpretation. The higher proportion of high-temperature rutiles in MN5 possibly indicates increased supply from the Seve Nappes, which locally reach granulite facies (Williams and Claesson 1998), and the increased abundance of metamafic rutiles is compatible with some supply from the Western Gneiss Region or adjacent areas of western Norway that contain metamafic rocks. The relatively high numbers of Type C garnet in MN5 sandstones (Figs. 3 and 4) also suggest some input from western Norway.

The two MN5 samples have markedly different garnet abundances due to burial-related dissolution, GZi being high (86.2) in the sample from well 6609/10-1 (1655.50 m) and low (0.5) in the sample from well 6506/11-1 (4436.00 m). Despite these differences, the rutile populations are closely comparable, providing further evidence that rutile geochemistry can be used to establish provenance characteristics of diagenetically modified sandstones.

DISCUSSION AND CONCLUSIONS

Detrital rutile geochemistry has proved to be a powerful additional tool for discriminating and characterising provenance of Jurassic-Paleocene sandstones in the Norwegian Sea. Four of the five sand types that have been previously distinguished using a combination of provenance-sensitive heavy-mineral ratios, garnet and tourmaline geochemistry and detrital-zircon age data (Morton et al. 2005b; Morton et al. 2009) can also be discriminated on the basis of the rutile data (Fig. 11, Table 1). MN3 sandstones are distinctive in having high abundances of metamafic rutiles, and rutiles in MN4 sandstones have characteristically high (granulite-facies) formation temperatures. MN2a sandstones have predominantly upper-amphibolite-facies rutiles, whereas MN1 and MN5 rutiles mainly fall in the lower-amphibolite-facies range. MN2a and MN4 sandstones (both derived from East Greenland) have lower proportions of metamafic rutiles than MN1, MN3 and MN5, which were sourced from Norway. The only two sand types that are less readily distinguishable on the basis of the rutile data are MN1 and MN5, believed to have been derived from adjacent parts of the Caledonian Nappe Domain of Mid-Norway. This paper therefore demonstrates that rutile geochemistry is a powerful provenance tool that is equally effective as other more well-established heavy-mineral provenance techniques, such as determination of provenance-

sensitive heavy-mineral ratios, garnet and tourmaline geochemistry, and detrital-zircon age dating.

Another important outcome of the study is that for each pair of samples, rutile compositions appear to be consistent (Fig. 11, Table 1). The two MN3 samples have similar proportions of metamafic and metapelitic rutiles, and the two MN4 samples have comparable temperature distributions, both peaking in the 800-850^{o}C bracket. Likewise, the temperature distributions for the two MN2a samples both peak in the 650-750^{o}C range, both the MN5 samples have peaks in the 550-650^{o}C range, and the two MN1 samples group between 550^{o}C and 700^{o}C. It is particularly noteworthy that the MN4 rutile populations indicate the presence of widespread granulite-facies metapelitic rocks, consistent with previous interpretations made on the basis of garnet geochemical data. Rutile geochemical analysis therefore has the potential to provide important provenance information on sandstones that have undergone extensive modification to their heavy-mineral suites, during either burial diagenesis or surficial weathering, precluding the use of other key parameters such as the garnet:zircon ratio (GZi) and garnet geochemistry.

Of the five sand types, MN1 and MN3 show the largest differences between the sample pairs, mainly manifested by the temperature plots. The rutiles in the MN1 sample from well 6710/10-1 have slightly lower temperatures (peaking at 550-650^{o}C) compared with those from well 6507/2-3 (peaking at 600-700^{o}C). One of the MN3 samples (from well 6305/8-1) has a bimodal temperature distribution, whereas the other (from well 35/3-5) is unimodal. It may be significant that the largest differences are shown by the two mineral pairs with the greatest spread of geographical locations (Fig. 1) and ages (the MN1 samples being Cenomanian and Paleocene, and the MN3 samples being Albian and Paleocene). The most

likely explanations of the observed differences are that they relate to geographical variations in the source areas, or to unroofing. Further rutile geochemical analyses are required to investigate these possibilities. Whatever the reason for these differences, the available data suggest that it may be possible to use rutile geochemistry to differentiate sandstone subtypes, thereby providing increased sophistication to the understanding of sediment provenance and intrabasinal distribution.

The pioneering work on the Zr-in-rutile geothermometer was based on the assumption that the rutile source rocks have a stable rutile-quartz-zircon assemblage (Zack et al., 2004a; Zack et al., 2004b), characteristic of metapelitic rocks. However, in this study, the temperature distributions for the metamafic rutiles mirror those of the metapelitic varieties, suggesting that for the most part, temperature estimates can be reliably acquired for both metapelitic and metamafic rutiles. The similarity in temperature distributions for metapelitic and metamafic rutiles is most convincingly demonstrated by the MN3 sample from well 6305/8-1 (Fig. 11). This sample has a bimodal temperature distribution that is shown by both the metapelitic and metamafic varieties, each peaking in the same two temperature brackets (600-650^{o}C and 700-750^{o}C). Meinhold et al. (2008) came to the same conclusion regarding reliability of temperature estimates from metamafic rutiles.

This case study integrating rutile geochemistry with more well-established provenance techniques has shown that rutile data provide additional information that constrains the nature of the ultimate source rocks. MN1 rutiles were ultimately derived from amphibolite-facies rocks of the Caledonian Nappe Domain of Nordland (northern Mid-Norway), with MN5 rutiles from similar sources slightly farther south. Both MN1 and MN5 rutile populations diagnose the involvement of subordinate metamafic rocks, compatible with the presence of

metamafic rocks within parts of the Caledonian Nappes. MN3 rutiles are dominated by amphibolite- or eclogite-facies metamafic varieties, consistent with a source in the Western Gneiss Region and adjacent parts of the Caledonian Nappe Domain. MN2a and MN4 rutile assemblages were mainly derived from metapelitic rocks of East Greenland, with MN2a being derived mainly from upper-amphibolite-facies rocks (probably the Nathorst Land Group) and MN4 from granulite-facies rocks (probably the Krummedal sequence).

This study, together with the pioneering work of Zack et al. (2004b), Stendal et al. (2006), Triebold et al. (2007), and Meinhold et al. (2008), demonstrates the considerable potential of rutile geochemistry as a provenance tracer. The combination of this technique with conventional heavy-mineral analysis, mineral-chemical analysis of other components of the heavy-mineral assemblages, and detrital-mineral geochronology will undoubtedly lead to more rigorous and accurate reconstructions of sediment provenance, paleogeography, and tectonic evolution of sediment source areas.

ACKNOWLEDGMENTS

We thank the sponsors of the CASP Norwegian Sea Provenance Project (BP, Chevron, ConocoPhillips, Shell, and StatoilHydro) for permission to use samples and information discussed in this paper, and to BP for permission to use samples and data from well 6305/8-1. We are grateful to Maria Mange, Guido Meinhold, Gene Rankey, and Andy Whitham for their constructive comments on this manuscript. SC publishes with permission of the Executive Director, British Geological Survey (NERC). The supplementary data described in this paper have been archived, and are available in digital form, at the Journal of Sedimentary Research Data Archive (URL: http://www.sepm.org/jsr/jsr_data_archive.asp).

REFERENCES

Asiedu, D.K., Suzuki, S., and Shibata, T., 2000, Provenance of sandstones from the Lower Cretaceous Sasayama Group, Inner Zone of Southwest Japan: Sedimentary Geology, v. 131, p. 9-24.

Belousova, E.A., Griffin, W.L., O'Reilly, S.Y., and Fisher, N.I., 2002a, Igneous zircon: trace element composition as an indicator of source rock type: Contributions to Mineralogy and Petrology, V. 143, p. 602-622.

Belousova, E.A., Griffin, W.L., O'Reilly, S.Y., and Fisher, N.I., 2002b, Apatite as an indicator mineral for mineral exploration: trace-element compositions and their relationship to host rock type: Journal of Geochemical Exploration, v. 76, p.45-69.

Brekke, H., Dahlgren, S., Nyland, B., and Magnus, C., 1999, The prospectivity of the Vøring and Møre basins on the Norwegian Sea continental margin, *in* Fleet, A.J., and Boldy, S.A.R., eds, Petroleum Geology of Northwest Europe: Proceedings of the 5th Conference: Geological Society of London, p. 261-274.

Cawood, P.A., 1983, Modal composition of detrital clinopyroxene geochemistry of lithic sandstones from the New England fold belt (East Australia): a Palaeozoic forearc terrane: Geological Society of America Bulletin, v. 94, p. 1199-1214.

Chenery, S., Cook, J.M., Styles, M., and Cameron, E.M., 1995, Determination of the three-dimensional distributions of precious metals in sulfide minerals by laser ablation microprobe-inductively coupled plasma-mass spectrometry (LAMP-ICP-MS): Chemical Geology, v. 124, p. 55-65.

Corfield, S., Sharp, I., Häger, K.-O., Dreyer, T., and Underhill, J., 2001, An integrated study of the Garn and Melke formations (Middle to Upper Jurassic) of the Smørbukk area, Halten Terrace, mid-Norway, *in* Martinsen, O.J., and Dreyer, T., eds, Sedimentary Environments Offshore Norway - Paleozoic to Recent: Norwegian Petroleum Society, Special Publication 10, p. 199-210.

Dalland, A., Worsley, D., and Ofstad, K., 1988. A lithostratigraphic scheme for the Mesozoic and Cenozoic succession offshore mid- and northern Norway: Norwegian Petroleum Directorate Bulletin, v. 4, p. 1-65.

Deer, W.A., Howie, R.A., and Zussman, J., 1992, An Introduction to the Rock-Forming Minerals, Second Edition: Harlow, U.K., Pearson Education Ltd, 712 p.

Dhuime, B., Bosch, D., Bruguier, O., Cabya, R., and Pourtales, S., 2007, Age, provenance and post-deposition metamorphic overprint of detrital zircons from the Nathorst Land group (NE Greenland) - A LA-ICP-MS and SIMS study: Precambrian Research, v. 155, p. 24-46.

Doré, A.G., Lundin, E.R., Jensen, L.N., Birkeland, Ø, Eliassen, P.E., and Fichler, C., 1999, Principal tectonic events in the evolution of the northwest European Atlantic margin, *in* Fleet,

A.J., and Boldy, S.A.R., eds, Petroleum Geology of Northwest Europe: Proceedings of the 5th Conference: Geological Society of London, p. 41-61.

Escher, J.C., and Pulvertaft, T.C.R., 1995, Geological map of Greenland, 1:2,500,000: Copenhagen, Geological Survey of Greenland.

Fonneland, H.C., Lien, T., Martinsen, O.J., Pedersen, R.B., and Kosler, J., 2004, Detrital zircon ages: a key to understanding the deposition of deep marine sandstones in the Norwegian Sea: Sedimentary Geology, v. 164, p. 147-159.

Force, E.R., 1980, The provenance of rutile: Journal of Sedimentary Petrology, v. 50, p. 485-488.

Force, E.R., 1991, Geology of Titanium-Mineral Deposits: Geological Society of America, Special Paper 259, 112 p.

Gaál, G., and Gorbatschev, R., 1987, An outline of the Precambrian evolution of the Baltic Shield: Precambrian Research, v. 35, p. 15-52.

Gjelberg, J.G., Enoksen, T., Kjaernes, P., Mangerud, G., Martinsen, O.J., Roe, E., and Vågnes, E., 2001, The Maastrichtian and Danian depositional setting along the eastern margin of the Møre Basin (mid-Norwegian Shelf): implications for reservoir development of the Ormen Lange Field, *in* Martinsen, O.J., and Dreyer, T., eds, Sedimentary Environments Offshore Norway - Palaeozoic to Recent: Norwegian Petroleum Society, Special Publication 10, p. 421-449.

Harley, S.L., 1998, On the occurrence and characterization of ultrahigh-temperature crustal metamorphism, *in* Treloar, P.J., and O'Brien, P.J., eds, What Drives Metamorphism and Metamorphic Reactions?: Geological Society of London, Special Publication 138, p. 81-107.

Harris, N.B., 1989, Reservoir geology of Fangst Group (Middle Jurassic), Heidrun Field, offshore Mid-Norway: American Association of Petroleum Geologists Bulletin, v. 73, p. 1415–1435.

Henry, D.J., and Guidotti, C.V., 1985, Tourmaline as a petrogenetic indicator mineral: an example from the staurolite-grade metapelites of NW Maine: American Mineralogist, v. 70, p. 1-15.

Hubert, J.F., 1962, A zircon-tourmaline-rutile maturity index and the interdependence of the composition of heavy mineral assemblages with the gross composition and texture of sandstones: Journal of Sedimentary Petrology, v. 32, p. 440-450.

Kalsbeek, F., Thrane, K., Nutman, A.P., and Jepsen, H.F., 2000, Late Mesoproterozoic to early Neoproterozoic history of the East Greenland Caledonides: evidence for Grenvillian orogenesis? Geological Society of London, Journal, v. 157, p. 1215-1225.

Kittilsen, J.E., Olsen, R.R., Marten, R.F., Hansen, E.K., and Hollingsworth, R.R., 1999, The first deepwater well in Norway and its implications for the Upper Cretaceous play, Vøring Basin, *in* Fleet, A.J., and Boldy, S.A.R., eds, Petroleum Geology of Northwest Europe: Proceedings of the 5th Conference: Geological Society of London, p. 275-280.

Kjaerefjord, J.M., 1999, Bayfill successions in the Lower Jurassic Åre Formation, offshore Norway: sedimentology and heterogeneity based on subsurface data from the Heidrun Field and analog data from the Upper Cretaceous Neslen Formation, eastern Book Cliffs, *in* Hentz, T.F., ed., Advanced Reservoir Characterisation for the 21st Century: Gulf Coast Section SEPM, Special Publication, 19th Annual Research Conference, p. 149-157.

Koistinen, T., Stephens, M.B., Bogatchev, V., Nordgulen, Ø., Wennerström, M., and Korhonen, J., 2001, Geological Map of the Fennoscandian Shield, Scale 1:2,000,000: Geological Surveys of Finland, Norway and Sweden and the North-West Department of Natural Resources of Russia.

Lonergan, L., and Mange-Rajetzky, M.A., 1994, Evidence for Internal Zone unroofing from foreland basin sediments, Betic Cordillera, SE Spain: Geological Society of London, Journal, v. 151, p. 515-529

McIlroy, D., 2004, Ichnofabrics and sedimentary facies of a tide-dominated delta: Jurassic Ile Formation of Kristin Field, Haltenbanken, offshore Mid-Norway, *in* McIlroy, D., ed., The Application of Ichnology to Palaeoenvironmental and Stratigraphic Analysis. Geological Society of London, Special Publication 228, p. 237-272.

Mange, M.A., and Morton, A.C., 2007, Geochemistry of heavy minerals, *in* Mange, M., and Wright, D.T., eds, Heavy Minerals In Use: Amsterdam, Elsevier, Developments in Sedimentology, v. 58, p. 345-391.

Mange-Rajetzky, M.A., and Oberhänsli, R., 1982, Detrital lawsonite and blue sodic amphibole in the Molasse of Savoy, France and their significance in assessing Alpine evolution: Schweizerische Mineralogische und Petrographische Mitteilungen, v. 62, p. 415-436.

Martinius, A., Kaas, I., Naess, A., Helgesen, G., Kjaerefjord, J., and Leith, D., 2001, Sedimentology of the heterolithic and tide-dominated Tilje Formation (Early Jurassic, Halten Terrace, offshore mid-Norway), *in* Martinsen, O.J., and Dreyer, T., eds, Sedimentary Environments Offshore Norway - Paleozoic to Recent. Norwegian Petroleum Society, Special Publication 10, p. 103-144.

Martinius, A.W., Ringrose, P.S., Brostrøm, C., Elfenbein, C., Naess, A., and Ringås, J.E., 2005, Reservoir challenges of heterolithic tidal sandstone reservoirs in the Halten Terrace, mid-Norway: Petroleum Geoscience, v. 11, p. 3-16.

Meinhold, G, Anders, B, Kostopoulos, D., and Reischmann, T., 2008, Rutile chemistry and thermometry as provenance indicator: An example from Chios Island, Greece: Sedimentary Geology, v. 203, .p 98-111.

Morton, A.C., 1985, A new approach to provenance studies: electron microprobe analysis of detrital garnets from Middle Jurassic sandstones of the northern North Sea: Sedimentology, v. 32, p. 553-566.

Morton, A.C., 1991, Geochemical studies of heavy minerals and their application to provenance research, *in* Morton, A.C., Todd, S.P., and Haughton, P.D.W., eds, Developments

in Sedimentary Provenance Studies: Geological Society of London, Special Publication 57, p. 31-45.

Morton, A.C., and Grant, S., 1998, Cretaceous depositional systems in the Norwegian Sea: heavy mineral constraints: American Association of Petroleum Geologists Bulletin, v. 82, p. 274-290.

Morton, A.C., and Hallsworth, C.R., 1994, Identifying provenance-specific features of detrital heavy mineral assemblages in sandstones: Sedimentary Geology, v. 90, p. 241-256.

Morton, A.C., and Hallsworth, C.R., 1999, Processes controlling the composition of heavy mineral assemblages in sandstones: Sedimentary Geology, v. 124, p. 3-29.

Morton, A.C., and Hallsworth, C.R., 2007, Stability of detrital heavy minerals during burial diagenesis, *in* Mange, M., and Wright, D.T., eds, Heavy Minerals In Use: Amsterdam, Elsevier, Developments in Sedimentology, v. 58, p. 215-245.

Morton, A.C., and Yaxley G., 2007, Detrital apatite geochemistry and its application in provenance studies, *in* Arribas, J., Critelli, S., and Johnsson, M.J., eds, Sediment Provenance and Petrogenesis: Perspectives from Petrography and Geochemistry: Geological Society of America, Special Paper 420, p. 319-344.

Morton, A.C., Hallsworth, C.R., and Chalton, B., 2004, Garnet compositions in Scottish and Norwegian basement terrains: a framework for interpretation of North Sea sandstone provenance: Marine and Petroleum Geology, v. 21, p. 393-410.

Morton, A.C., Hallsworth, C.R., Strogen, D., Whitham, A.G., and Fanning, C.M., 2009, Evolution of provenance in the NE Atlantic rift: the Early-Middle Jurassic succession in the Heidrun Field, Halten Terrace, offshore Mid Norway: Marine and Petroleum Geology, in press.

Morton, A.C., Whitham, A.G., and Fanning, C.M., 2005a, Provenance of Late Cretaceous-Paleocene submarine fan sandstones in the Norwegian Sea: integration of heavy mineral, mineral chemical and zircon age data: Sedimentary Geology, v. 182, p. 3-28.

Morton, A.C., Whitham, A.G., Fanning, C.M., and Claoué-Long, J.C., 2005b, The role of East Greenland as a source of sediment to the Vøring Basin during the Late Cretaceous, *in* Wandås, B.T.G., Eide, E.A., Gradstein, F., and Nystuen J.P., eds, Onshore-Offshore Relationships on the North Atlantic Margin: Norwegian Petroleum Society, Special Publication 12, p. 83-110.

Owen, M.R., 1987, Hafnium content of detrital zircons, a new tool for provenance study: Journal of Sedimentary Petrology, v. 57, p. 824-830.

Pearce, N.J.G., Perkins, W.T., Westgate, J.A., Gorton, M.P., Jackson, S.E., Neal, C.R., and Chenery, S., 1997, A compilation of new and published major and trace element data for NIST SRM610 and NIST SRM612 glass reference materials: Geostandards Newsletter – The Journal of Geostandards and Geoanalysis, v. 21, p. 115-144.

Peucat, J.J., Tisserant, D., Caby, R., and Clauer, N., 1985, Resistance of zircons to U–Pb resetting in a prograde metamorphic sequence of Caledonian age in East Greenland: Canadian Journal of Earth Sciences, v. 22, p. 330-338.

Pober, E., and Faupl, P., 1988, The chemistry of detrital chrome spinels and its implications for the geodynamic evolution of the Eastern Alps: Geologische Rundschau, v. 77, p. 641-670.

Preston, R.J., Hartley, A., Hole, M.J., Buck, S., Bond, J., Mange-Rajetzky, M., and Still, J., 1998, Integrated whole-rock trace element geochemistry and heavy-mineral chemistry studies: aids to the correlation of continental red-bed reservoirs in the Beryl Field, U.K. North Sea: Petroleum Geoscience, v. 4, p. 7-16.

Preston, J., Hartley, A., Mange-Rajetzky, M., Hole, M.J., May, G., and Buck, S., 2002, The provenance of Triassic continental sandstones from the Beryl Field, northern North Sea: mineralogical, geochemical, and sedimentological constraints: Journal of Sedimentary Research, v. 72, p. 18-29.

Price, S.P., and Whitham, A.G., 1997, Exhumed hydrocarbon traps in East Greenland: analogs for the Lower-Middle Jurassic play of NW Europe: American Association of Petroleum Geologists Bulletin, v. 81, p. 196-221.

Qvale, H., and Stigh, J., 1985, Ultramafic rocks in the Scandinavian Caledonides, *in* Gee, D.G., and Sturt, B.A., eds, The Caledonide Orogen: Scandinavia and Related Areas: Chichester, U.K., Wiley, p. 693-715.

Roberts, D., 2003, The Scandinavian Caledonides: event chronology, palaeogeographic settings and likely modern analogues: Tectonophysics, v. 365, p. 283-299.

Sabeen, H.M., Ramanujam, N., and Morton, A.C., 2002, The provenance of garnet: constraints provided by studies of coastal sediments from Southern India: Sedimentary Geology, v. 152, p. 279-287.

Scott, R.A., 2000, Mesozoic-Cenozoic evolution of East Greenland: implications of a reinterpreted continent-ocean boundary location: Polarforschung, v. 68, p. 83-91.

Seidler, L., Steel, R.J., Stemmerik, L., and Surlyk, F., 2004, North Atlantic marine rifting in the Early Triassic: new evidence from East Greenland: Geological Society of London, Journal, v. 161, p. 583-592.

Shanmugam, G., Lehtonen, L.R., Straume, T., Syvertsen, S.E., Hodgkinson, R.J., and Skibeli, M., 1994, Slump and debris-flow dominated upper slope facies in the Cretaceous of the Norwegian and northern North Sea (61-67^{o}N): implications for sand distribution: American Association of Petroleum Geologists Bulletin, v. 78, p. 910-937.

Sigmond, E.N.O., 1992, Bedrock map of Norway and adjacent ocean area, 1:3,000,000: Oslo, Geological Survey of Norway.

Skår, Ø., 2002, U-Pb geochronology and geochemistry of early Proterozoic rocks of the basement windows in central Nordland, Caledonides of north-central Norway: Precambrian Research, v. 116, p. 265-283.

Spiegel, C., Siebel, W., Frisch, W., and Berner, Z., 2002, Nd and Sr isotopic ratios and trace element geochemistry of epidote from the Swiss Molasse Basin as provenance indicators: implications for the reconstruction of the exhumation history of the Central Alps: Chemical Geology, v. 189, p. 231-250.

Stemmerik, L., Christiansen, F.G., Piasecki, S., Jordt, B., Marcussen, C., and Nøhr-Hansen, H., 1993, Depositional history and petroleum geology of the Carboniferous to Cretaceous sediments in the northern part of East Greenland, *in* Vorren, T.O., Bergsager, E., Dahl-Stamnes, Ø.A., Holter, E., Johansen, B., Lie, E., and Lund, T.B., eds., Arctic Geology and Petroleum Potential: Norwegian Petroleum Society, Special Publication, v. 2, p. 67-87.

Stendal, H., Toteu, S.F., Frei, R., Penaye, J., Njel, U.O., Bassahak, J., Nni, J., Kankeu, B., Ngako, V., and Hell, J.V., 2006, Derivation of detrital rutile in the Yaoundé region from the Neoproterozoic Pan-African belt in southern Cameroon (Central Africa): Journal of African Earth Sciences, v. 44, p. 443-458.

Surlyk, F., 1990, Timing, style and sedimentary evolution of Late Paleozoic-Mesozoic extensional basins of East Greenland, *in* Hardman, R.P.F., and Brooks, J., eds., Tectonic Events Responsible for Britain's Oil and Gas Reserves: Geological Society of London, Special Publication 55, p. 107-125.

Svela, K.E., 2001, Sedimentary facies in the fluvial-dominated Åre Formation as seen in the Åre 1 member in the Heidrun Field, *in* Martinsen, O.J., and Dreyer, T., eds, Sedimentary

Environments Offshore Norway - Paleozoic to Recent: Norwegian Petroleum Society, Special Publication 10, p. 87-102.

Swiecicki, T., Gibbs, P., Farrow, G., and Coward, M.P., 1998, A tectonostratigraphic framework for the Mid-Norway region: Marine and Petroleum Geology, v. 15, p. 245-276.

Triebold, S., von Eynatten, H., Luvizotto, G.L., and Zack, T., 2007, Deducing source rock lithology from detrital rutile geochemistry: an example from the Erzgebirge, Germany: Chemical Geology, v. 244, p. 421-436.

Turner, G., and Morton, A.C., 2007, The effects of burial diagenesis on detrital heavy mineral grain surface textures, in Mange, M., and Wright, D.T., eds, Heavy Minerals In Use: Amsterdam, Elsevier, Developments in Sedimentology, v. 58, p. 393-412.

Vergara, L., Wreglesworth, I., Trayfoot, M., and Richardson, G., 2001, The distribution of Cretaceous and Paleocene deep-water reservoirs in the Norwegian Sea basins: Petroleum Geoscience, v. 7, p. 395-408.

Walderhaug, O., and Porten, K.W., 2007, Stability of detrital heavy minerals on the Norwegian continental shelf as a function of depth and temperature: Journal of Sedimentary Research, v. 77, p. 992-1002.

Watson, E.B., Wark, D.A., and Thomas, J.B., 2006, Crystallization thermometers for zircon and rutile: Contributions to Mineralogy and Petrology, v. 151, p. 413-433.

White, A.P., Hodges, K.V., and Martin, M.W., 2002, Geologic constraints on middle-crustal behavior during broadly synorogenic extension in the central East Greenland Caledonides: International Journal of Earth Sciences, v. 91, p. 187-208.

Whitham, A.G., Morton, A.C., and Fanning, C.M., 2004, Insights into Paleocene sediment transport paths and basin evolution in the North Atlantic from a heavy mineral study of sandstones from southern East Greenland: Petroleum Geoscience, v. 10, p. 61-72.

Williams, I.S., and Claesson, S., 1987, Isotopic evidence for the Precambrian provenance and Caledonian metamorphism of high grade paragneisses from the Seve Nappes, Scandinavian Caledonides: Contributions to Mineralogy and Petrology, v. 97, p. 205-217.

Zack, T., Moraes, R., and Kronz, A., 2004a, Temperature dependence of Zr in rutile: empirical calibration of a rutile thermometer: Contributions to Mineralogy and Petrology, v. 148, p. 471-488.

Zack, T., von Eynatten, H., and Kronz, A., 2004b, Rutile geochemistry and its potential use in quantitative provenance studies: Sedimentary Geology, v. 171, p. 37-58.

Zack, T., Kronz, A., Foley, S.F., and Rivers, T., 2002, Trace element abundances in rutiles from eclogites and associated garnet mica schists: Chemical Geology, v. 184, p. 97-122.

FIGURE CAPTIONS

Fig. 1. Best-fit reconstruction of the Norwegian Sea prior to final opening of the northeast Atlantic (magnetic anomaly 24), adapted from Scott (2000), showing locations of wells discussed in this paper and inferred source areas for sand types MN1, MN2, MN3, MN4, and MN5 (from Morton et al. 2005a, Morton et al. 2005b, and Morton et al. 2009). Data sources for East Greenland and Norway geology are Gaál and Gorbatschev (1987), Sigmond (1992), Escher and Pulvertaft (1995), and Koistinen et al. (2001). Note that this map does not take Jurassic and Cretaceous extension in the Norwegian Sea into account. COB = continent-ocean boundary.

Fig. 2. Provenance-sensitive heavy-mineral ratios in sand types MN1, MN2a, MN3, MN4, and MN5 from wells discussed in this paper. RuZi = rutile:zircon index (% rutile in total rutile plus zircon), ATi = apatite:tourmaline index (% apatite in total apatite plus tourmaline), MZi = monazite:zircon index (% monazite in total monazite plus zircon), CZi = chrome spinel:zircon index (% chrome spinel in total chrome spinel plus zircon), as described by Morton and Hallsworth (1994).

Fig. 3. Representative garnet compositions in Norwegian Sea sand types MN1, MN2a, MN3, MN4 and MN5. Compositional fields for garnet types A, B, and C (as defined by Morton et al., 2004) are shown on the MN5 ternary plot.

X_{Fe}, X_{Mg}, X_{Ca}, X_{Mn} = ionic proportions of Fe, Mg, Ca, and Mn. All Fe calculated as Fe^{2+}.

● - $X_{Mn} < 5\%$. ○ - $X_{Mn} > 5\%$. ▲ - $Fe^{3+}/Al > 0.1$

MN1 = 6710/10-1, 1111.50 m (Tang Formation)

MN2a = 6706/11-1, 2315.30 m (Nise Formation)

MN3 = 6305/8-1, 2972.25 m (Tang Formation)

MN4 = 6507/8-4, 2258.95 m (Åre Formation)

MN5 = 6609/10-1, 1655.50 m (Tilje Formation)

Fig. 4. Relative abundances of garnet types A, B, and C (as defined by Morton et al. 2004, and shown in Fig. 3) in Norwegian Sea sand types MN1, MN2a, MN3, MN4, and MN5 from wells discussed in this paper.

Fig. 5. Representative tourmaline compositions in sand types MN1, MN2a, MN3, MN4, and MN5. Compositional fields (from Henry and Guidotti 1985) are as follows:

Field A - Li-rich granitoids, pegmatites and aplites. Field B - Li-poor granitoids, pegmatites, and aplites. Field C – hydrothermally altered granitic rocks. Field D - Aluminous metapelites and metapsammites. Field E - Al-poor metapelites and metapsammites. Field F - Fe^{3+}-rich quartz-tourmaline rocks, calc-silicates, and metapelites.

MN1 = 6507/2-3, 3261.00 m (Lange Formation)

MN2a = 6706/11-1, 3749.90 m (Nise Formation)

MN3 = 35/3-5, 3290.90 m (Agat Formation)

MN4 = 6507/8-4, 2258.95 m (Åre Formation)

MN5 = 6609/10-1, 1655.50 m (Tilje Formation)

Fig. 6. Relative abundances of tourmaline types D, E, and F (as defined by Henry and Guidotti 1985) in sand types MN1, MN2a, MN3, MN4, and MN5 from wells discussed in this paper.

Fig. 7. Relative probability plots of zircon age spectra for representative samples of MN1, MN2a, MN3, MN4, and MN5 sandstones, as determined by sensitive high resolution ion microprobe (SHRIMP).

MN1 = 6710/10-1, 1459.20 m, Tang Formation (from Morton et al. 2005b)

MN2a = 6607/5-2, 4172.00 m, Nise Formation (from Morton et al. 2005b)

MN3 = 6305/7-1, 2959.00 m, Tang Formation (from Morton et al. 2005a)

MN4 = 6507/8-4, 2202.60 m, Åre Formation (from Morton et al. 2009)

MN5 = 6507/8-1, 2456.90 m, Tilje Formation (from Morton et al. 2009)

Fig. 8. Plot of GZi against burial depth in sandstones from wells discussed in this paper. Encircled data points are the samples used for rutile geochemical analysis.

Fig. 9. Cr-Nb plots showing contrasting rutile provenance in two of the samples discussed in this paper. Discrimination of metamafic and metapelitic rutile is based on Meinhold et al. (2008). N = number of rutile grains analysed.

Fig. 10. Comparison of rutile formation temperatures using the Zr-in-rutile geothermometers of Zack et al. (2004a) and Watson et al. (2006) for the sample from well 6406/2-1, 4429.85 m, Garn Formation (sand type MN4).

T_Z = temperature using the Zack et al. (2004a) formula.

T_W = temperature using the Watson et al. (2006) formula.

Fig. 11. Relative abundance of metamafic and metapelitic rutiles (pie charts) and rutile formation temperatures (histograms) for MN1, MN2a, MN3, MN4, and MN5 sandstones. Temperatures were calculated using the Watson et al. (2006) formula.

APPENDIX: RUTILE GEOCHEMISTRY BY LASER ABLATION INDUCTIVELY COUPLED PLASMA MASS SPECTROMETRY

Sample preparation

Rutile grains were picked from heavy-mineral residues under the petrographic microscope, taking care to avoid grains containing large or numerous inclusions, and were mounted on double sided adhesive tape stuck to custom-made clear acrylic plastic (Perspex) slides. The tape and clear Perspex have previously been demonstrated to have insignificant trace-element contents. This mounting method overcomes the risk of contamination that might be encountered while drilling through fragile or small rutile grains into normal glass slides. Approximately 50 rutile grains were analyzed per sample.

The BGS LA-ICP-MS system

The British Geological Survey (BGS) laser ablation microprobe consists of a Spectron Nd:YAG laser operating in the far-UV (266 nm), linked to a high-quality Leitz microscope and is reported in UK Patent 9106337.0, Serial 2254444, 1992. A VG PlasmaQuad 2+ ICP mass spectrometer (Serial No: SLOT-732), with a modified sample introduction system (described below) was used in isotope peak jumping mode to achieve the best detection limits on a transient signal.

The rutile grain mount was placed in a Perspex cell under a 36x microscope lens. The sample can be illuminated in either transmitted light or reflected light as appropriate. After choosing the analytical area of interest and positioning this under the cross-wires, the laser was fired

through the microscope for 15-20 seconds. The ablated material was transported to the ICP-MS instrument by a continuous flow of argon gas through the Perspex cell and connecting tubing, which links into the inlet of the ICP torch.

In the ICP torch, the sample was vaporized and ionized by a hot (6000 K) argon plasma. The ionised material passed into the vacuum region of the mass spectrometer, where a quadrupole mass filter was used to select ions of an appropriate mass-to-charge ratio. The quadrupole can be rapidly scanned or peak jumped from masses as light as 7 (lithium) to uranium at mass 238. Ions passing through the quadrupole were detected by an electron multiplier and counted by a multi-channel analyzer. Since trace elements of medium to heavy mass (^{93}Nb to ^{238}U) were of particular interest in the current study, a modicum of additional vacuum pumping was applied to the region of the interface between the ICP and the mass spectrometer. This enhanced the sensitivity of the isotopes greater than mass 80, at the expense of the lighter isotopes, with the added advantage of keeping the measured ^{49}Ti isotope within the linear range of the detector

To overcome difficulties in optimizing the instrument when trying to measure transient signals from a pulse of laser-ablated material, a dual-gas-flow sample introduction system has been developed, in which flow from the ablation cell is merged with the carrier gas from a conventional nebulizer/spray chamber. These two gas flows are combined concentrically in a small glass mixer placed between the nebulizer and the torch. The advantage of this configuration is that it permits simultaneous introduction of laser-ablated solids and nebulized aqueous solutions, which then enter an identical bulk plasma environment. As a consequence, the ICP mass spectrometer can be tuned just as if solution nebulization were being performed (Chenery et al 1995). The instrument is calibrated using a glass standard

(NIST611) containing a large number of trace elements at a concentration of approximately 500 mg/kg (ppm). Exact values used are taken from Pearce et al. (1997).

It is necessary to use an internal standard to compensate for the poor reproducibility in the analytical signal caused by variations in the mass of the material ablated. This is normally a minor isotope of a major elemental component, the concentration of which is known from stoichiometry or determined by an independent analytical technique. In this work, the rutile was assumed to be stoichiometric with a calculated Ti concentration of 599499 mg/kg based on the atomic masses of Ti and O.

ICP mass spectrometry is a very sensitive analytical technique capable of determining a large number of elements at low concentrations. The best detection limits are achieved by ideally limiting the number of isotopes determined in any one acquisition to 12 to 20 and peak jumping just between those isotopes. In the current study, the element list was limited to: ^{24}Mg, ^{27}Al, ^{49}Ti, ^{51}V, ^{52}Cr, ^{55}Mn, ^{59}Co, ^{89}Y, ^{90}Zr, ^{93}Nb, ^{95}Mo, ^{139}La, ^{208}Pb, ^{232}Th, and ^{238}U.

Laser Ablation Sampling of the Test Materials

One of the fundamental principles of the LA-ICP-MS is that for a given set of operating parameters, the detection limits of the system are directly proportional to the mass of material sampled. Material can be sampled as discrete craters to achieve high spatial resolution; with the LA system used in the current study, crater sizes may be varied between 40 μm diameter and greater than 50 μm deep to smaller than 1 μm diameter and deep. However, this may not give enough material to yield the very best detection limits needed. For any particular piece of research a compromise may have to be struck between the desired spatial resolution and

the detection limits required. An alternative is to raster the laser beam over a small area of the sample surface, which additionally ensures that the laser does not penetrate too deeply into the grain. In the current study, where grains were from the 63-125 μm sieve fraction, it was possible to raster a 4 x 4 matrix of spots, a 10 μm gap between spots and a dwell time of 1 s at each spot, removing material over an area of approximately 50 μm x 50 μm.

Data Acquisition and Treatment

The following procedure was used for data acquisition and treatment:

1. Data were collected by the ICP-MS in a time-resolved fashion and were in raw response units for laser-ablated material. The ICP-MS response for any given isotope should be linear with respect to relative concentration. The data were transferred to an off-line computer running the Microsoft Excel spreadsheet package. The area under the peak for the individual laser ablations was calculated.

2. These data were then corrected by subtraction of a blank integration. This was calculated from data collected immediately before a group of ablations. The detection limits were also calculated from three standard deviations of the variation in blank signal.

3. To correct for differences in isotopic abundance, ionization efficiency, and differences in response due to mass, a calibration was performed using a glass standard of known concentration for each isotope. This calibration was applied to the responses from laser-ablated material. The modified data are in arbitrary concentration units (a.c.u.);

4. Finally, because the absolute amount of material ablated by the laser varies from shot to shot and the efficiency of sample introduction by laser ablation is different from that of a solution, a correction was made using an internal standard to calculate absolute concentrations. The rutile was assumed to be stoichiometric with a calculated Ti concentration of 599499 mg/kg.

Table 1. Summary of detrital rutile compositions

Well	6710/10-1	6507/2-3	6706/11-1	6706/11-1	35/3-5	6305/8-1	6406/2-1	6507/8-4	6609/10-1	6506/11-2
Depth (m)	1096.90	3261.00	2315.30	3749.90	3290.90	2972.25	4429.85	2258.95	1655.50	4436.05
Age	Pal	Cen	Cam	San	Alb	Pal	Baj-Bath	Sin-Het	Het-Plb	Baj
sand type	MN1	MN1	MN2a	MN2a	MN3	MN3	MN4	MN4	MN5	MN5
total rutiles analysed	48	51	52	50	48	52	54	54	51	51
metapelitic rutile %	69	76	87	96	40	38	89	76	76	67
metamafic rutile %	31	24	13	4	60	62	11	24	24	33
metapelitic rutiles %										
greenschist	2	0	0	2	0	0	0	0	0	6
lower amphibolite/ eclogite	48	47	8	8	23	17	2	4	51	35
upper amphibolite/ eclogite	17	29	62	70	15	12	9	4	20	14
granulite	2	0	17	16	2	10	74	69	6	12
metamafic rutiles %										
greenschist	15	0	0	0	6	2	0	2	0	2
lower amphibolite/ eclogite	10	10	2	0	38	29	0	4	16	18
upper amphibolite/ eclogite	6	6	8	4	15	17	0	4	4	4
granulite	0	8	4	0	2	13	15	15	4	10

Pal = Paleocene, Cam = Campanian, San = Santonian, Cen = Cenomanian, Alb = Albian, Bath = Bathonian, Baj = Bajocian, Plb = Pliensbachian, Sin = Sinemurian, Het = Hettangian

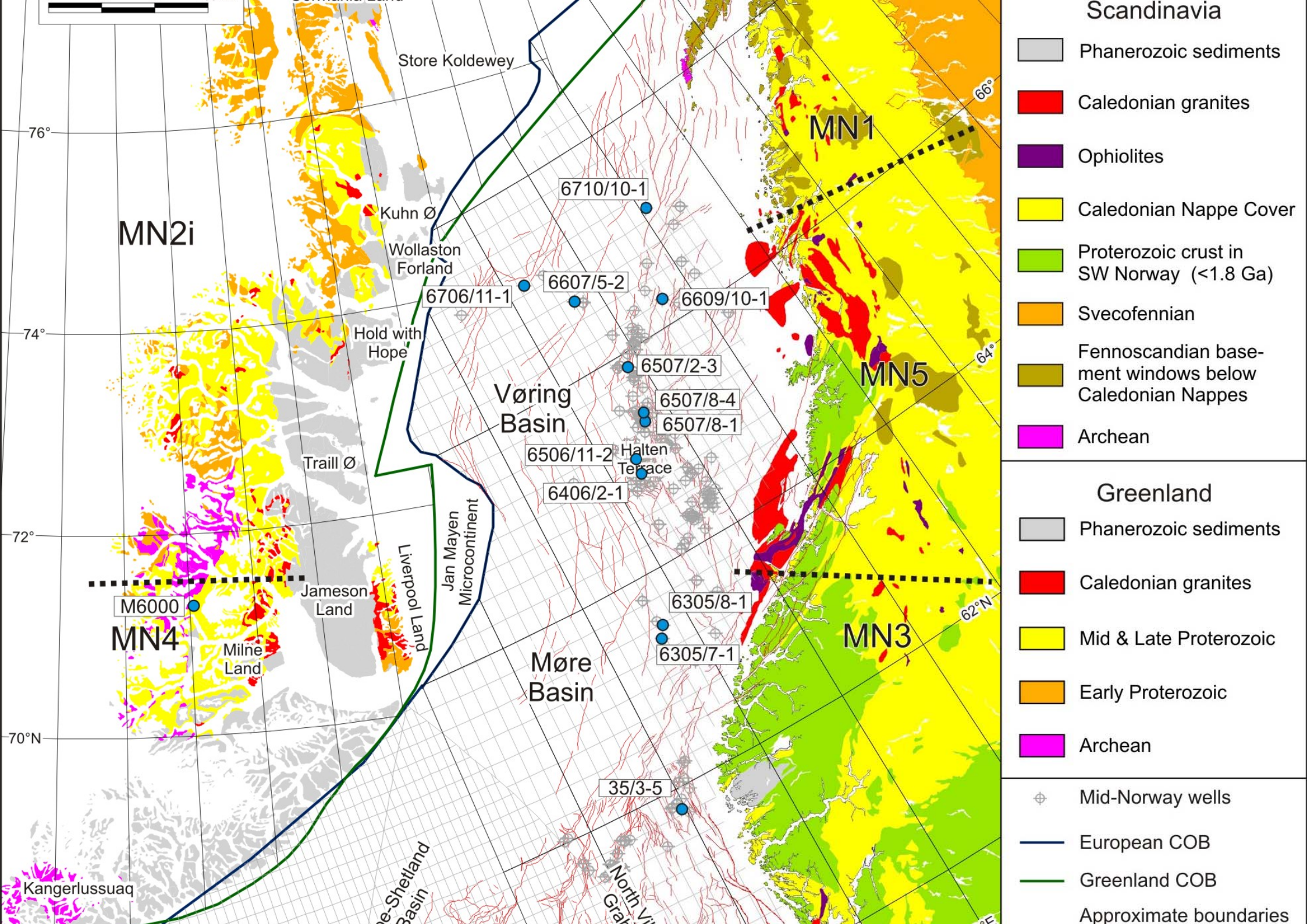
Store Koldewey
76°
MN2i
Kuhn Ø
Wollaston Forland
6710/10-1
6706/11-1
6607/5-2
6609/10-1
74°
Hold with Hope
6507/2-3
Vøring Basin
6507/8-4
6507/8-1
Traill Ø
6506/11-2
Halten Terrace
6406/2-1
Jan Mayen Microcontinent
Liverpool Land
72°
M6000
MN4
Jameson Land
Milne Land
6305/8-1
6305/7-1
Møre Basin
70°N
35/3-5
Kangerlussuaq
MN1
MN5
MN3
66°
64°
62°N
Scandinavia
Phanerozoic sediments
Caledonian granites
Ophiolites
Caledonian Nappe Cover
Proterozoic crust in SW Norway (<1.8 Ga)
Svecofennian
Fennoscandian base-ment windows below Caledonian Nappes
Archean
Greenland
Phanerozoic sediments
Caledonian granites
Mid & Late Proterozoic
Early Proterozoic
Archean
Mid-Norway wells
European COB
Greenland COB
Approximate boundaries

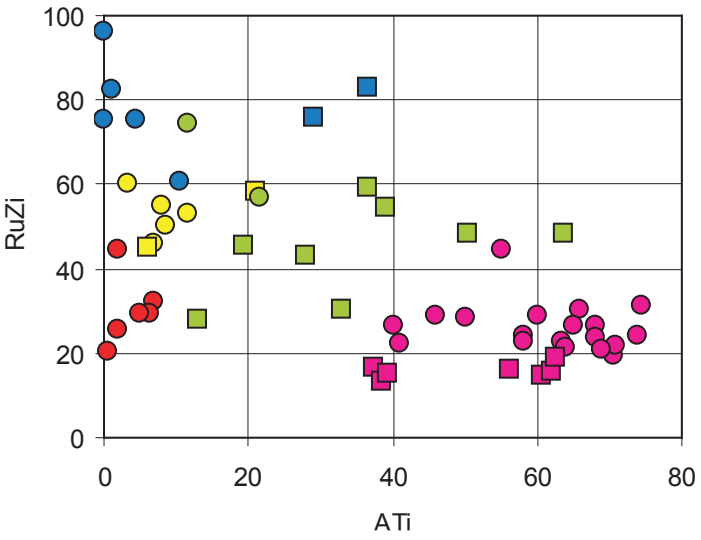

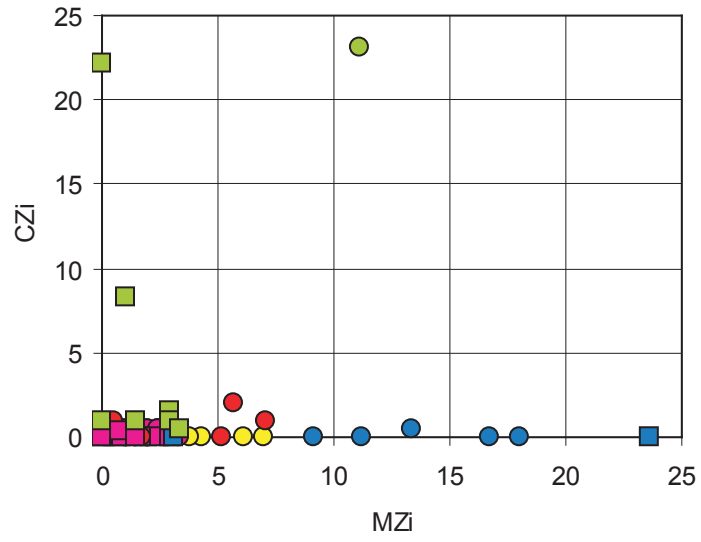

MN1, 6710/10-1 MN1, 6507/2-3 MN2a, 6706/11-1
MN3, 6305/8-1 MN3, 35/3-5 MN4, 6507/8-4
MN4, 6406/2-1 MN5, 6609/10-1 MN5, 6506/11-2

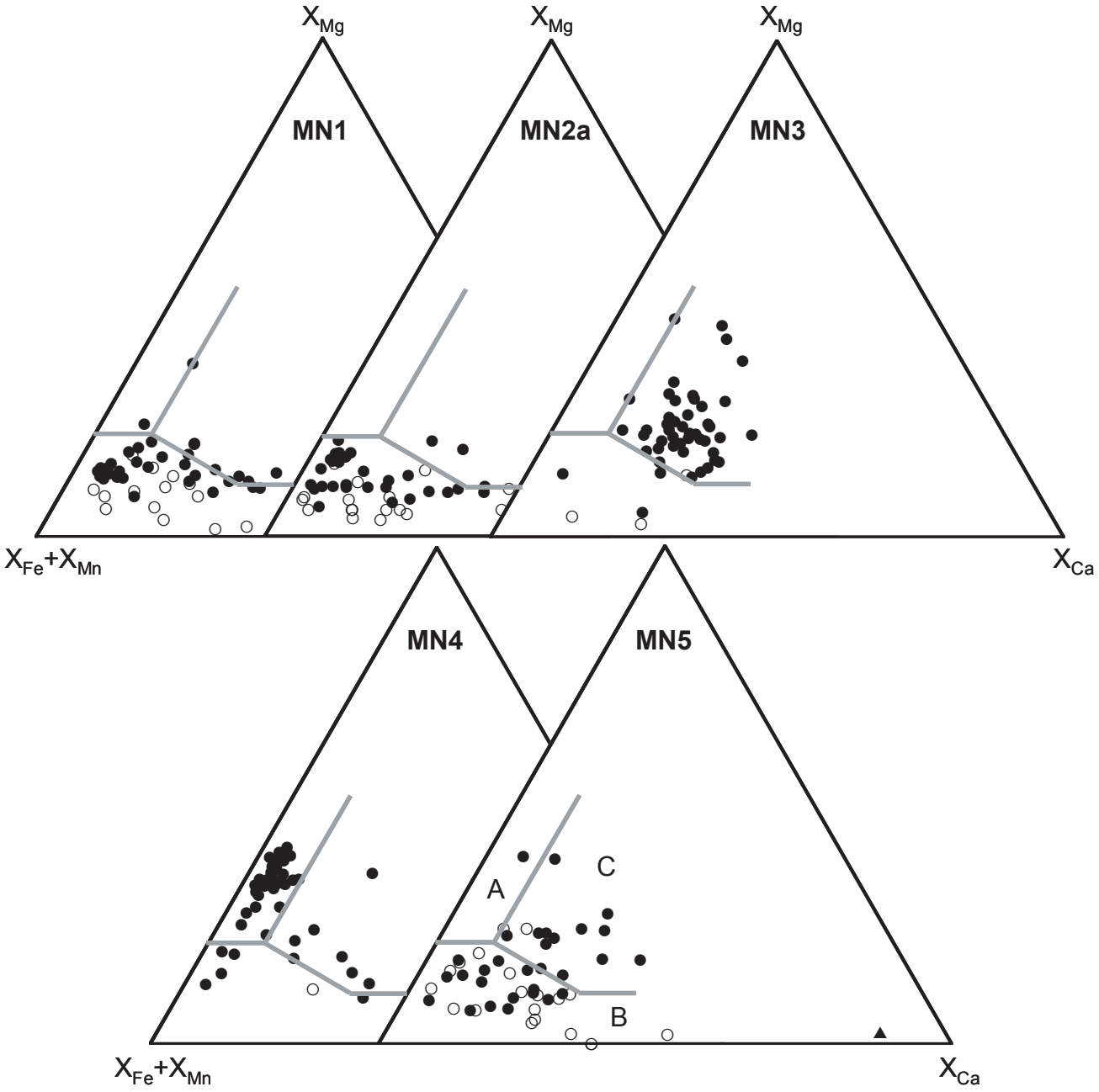
X_Mg
X_Mg
X_Mg
MN1
MN2a
MN3
X_Fe+X_Mn
X_Ca
MN4
MN5
A
B
C
X_Fe+X_Mn
X_Ca

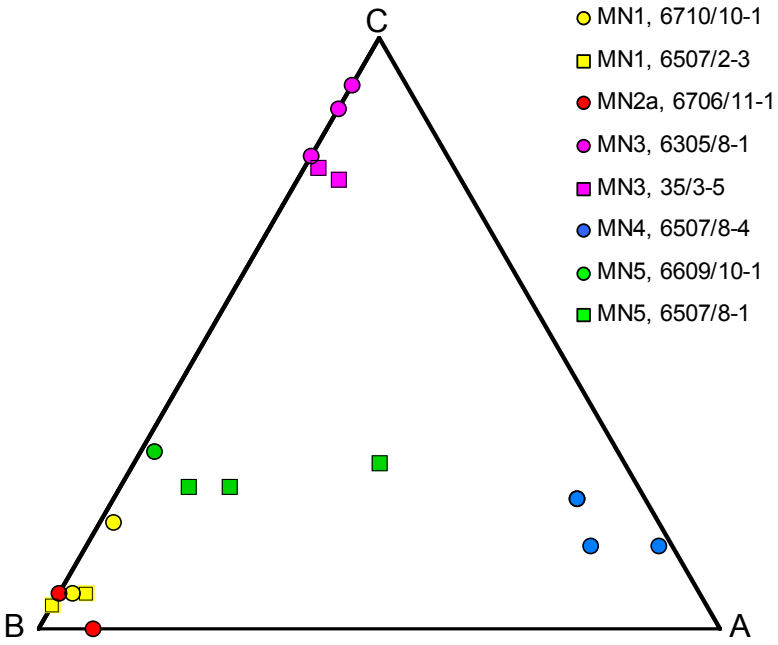
C
B
A
MN1, 6710/10-1
MN1, 6507/2-3
MN2a, 6706/11-1
MN3, 6305/8-1
MN3, 35/3-5
MN4, 6507/8-4
MN5, 6609/10-1
MN5, 6507/8-1

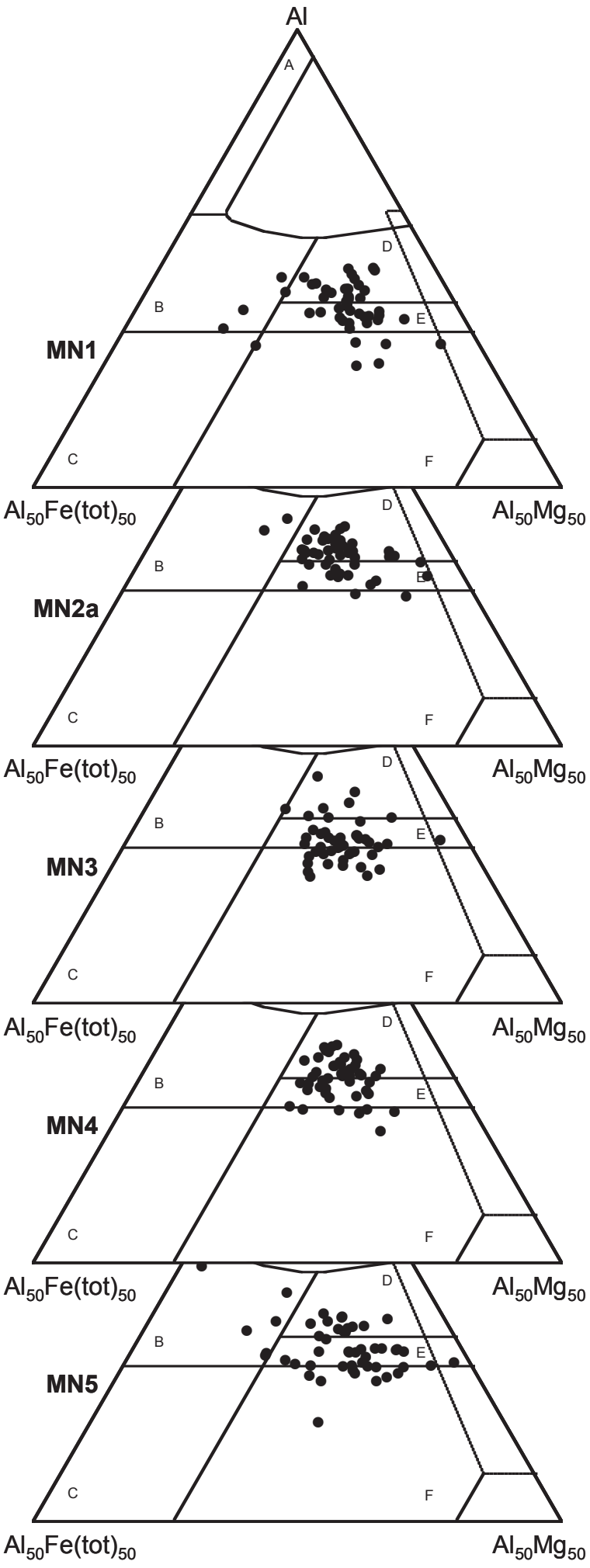
Al
A
D
B
E
MN1
C
F
Al50Fe(tot)50
Al50Mg50
D
B
E
MN2a
C
F
Al50Fe(tot)50
Al50Mg50
D
B
E
MN3
C
F
Al50Fe(tot)50
Al50Mg50
D
B
E
MN4
C
F
Al50Fe(tot)50
Al50Mg50
D
B
E
MN5
C
F
Al50Fe(tot)50
Al50Mg50

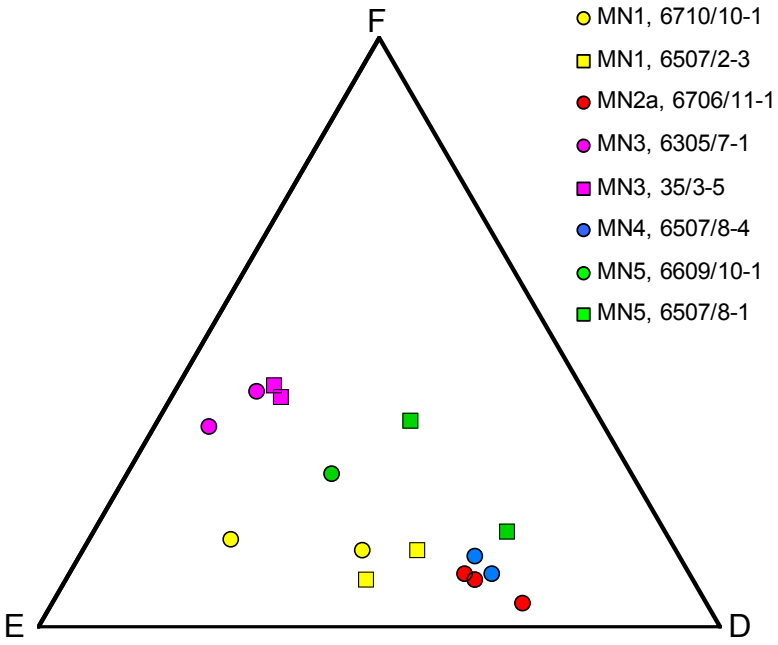
F
E
D
MN1, 6710/10-1
MN1, 6507/2-3
MN2a, 6706/11-1
MN3, 6305/7-1
MN3, 35/3-5
MN4, 6507/8-4
MN5, 6609/10-1
MN5, 6507/8-1

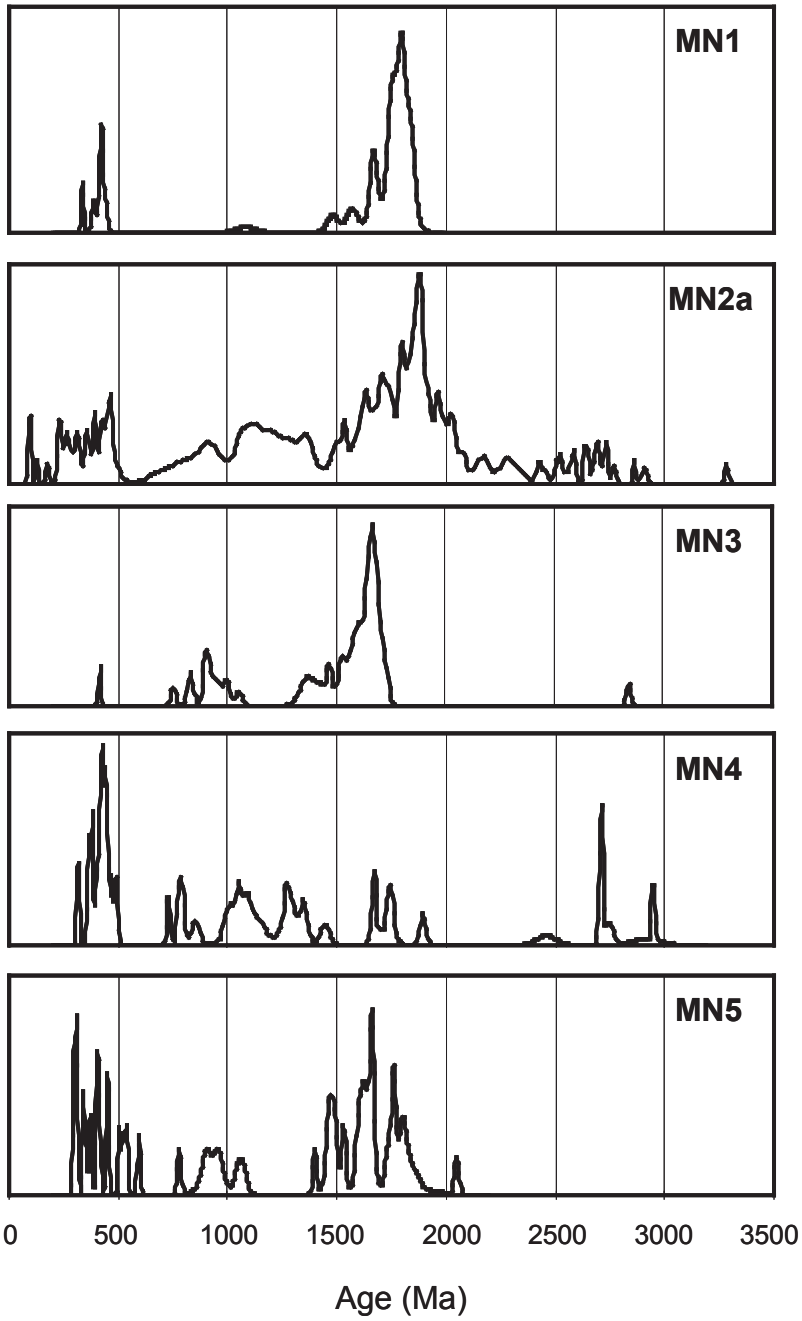
MN1
MN2a
MN3
MN4
MN5
0
500
1000
1500
2000
2500
3000
3500
Age (Ma)

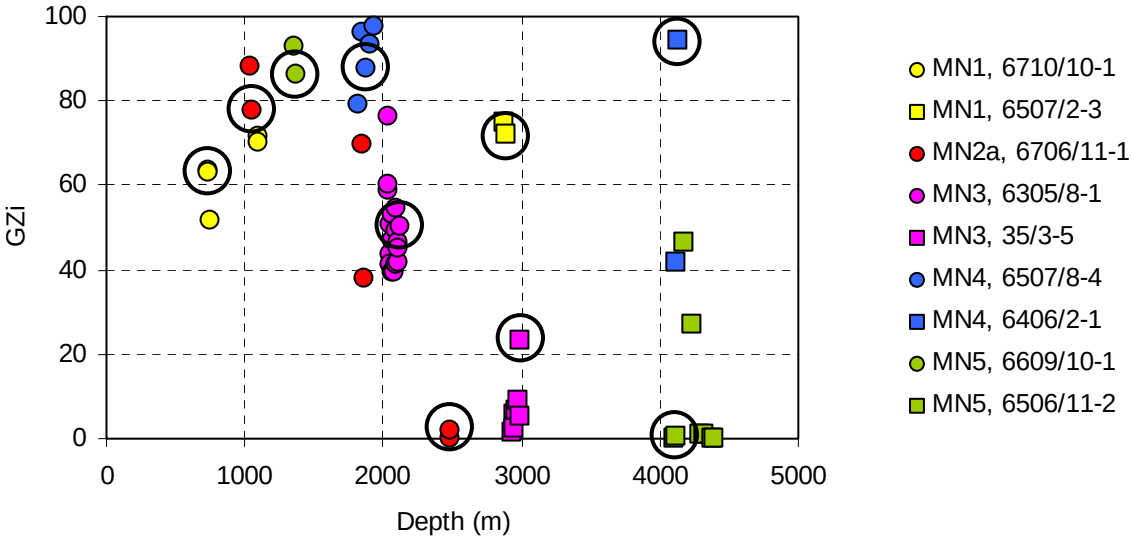
100
80
60
40
20
0
GZi
0
1000
2000
3000
4000
5000
Depth (m)
MN1, 6710/10-1
MN1, 6507/2-3
MN2a, 6706/11-1
MN3, 6305/8-1
MN3, 35/3-5
MN4, 6507/8-4
MN4, 6406/2-1
MN5, 6609/10-1
MN5, 6506/11-2

Fig. 8

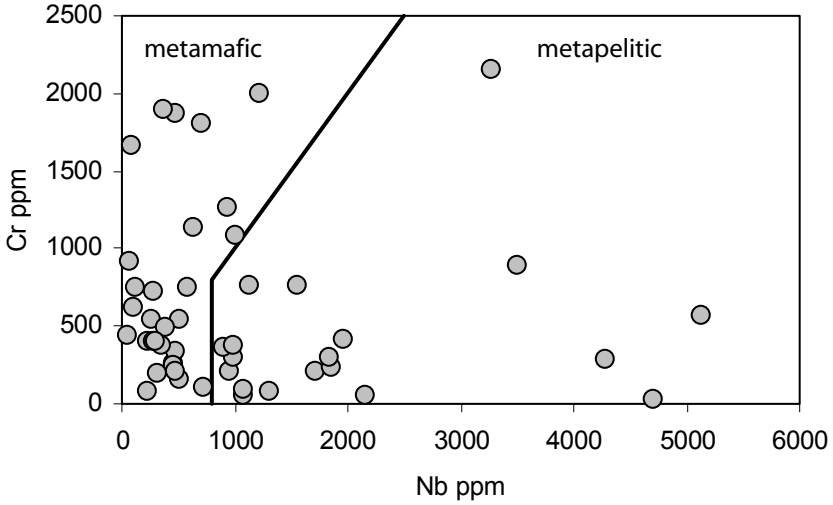

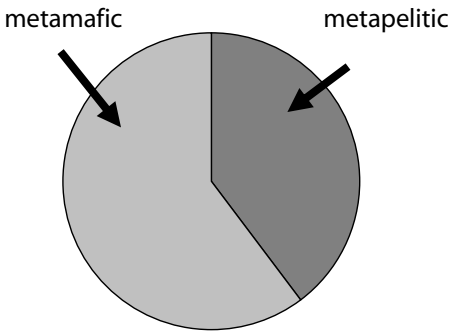

35/3-5, 3290 90 m
Agat Formation (sand type MN3)

N = 48

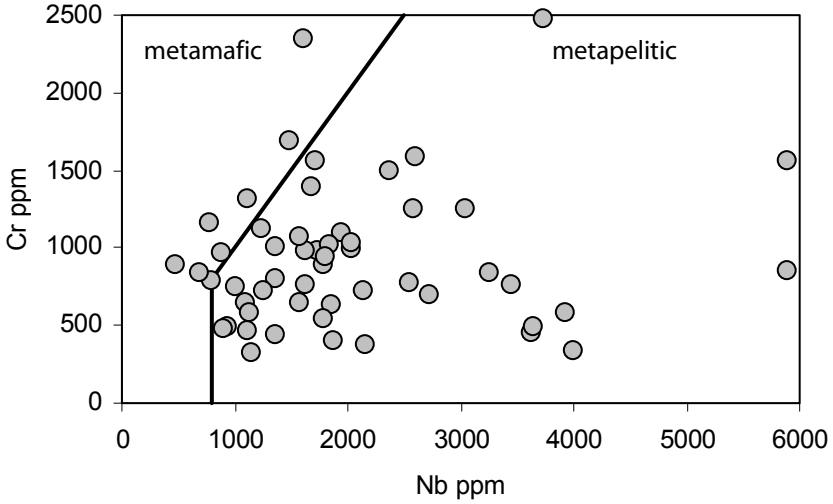

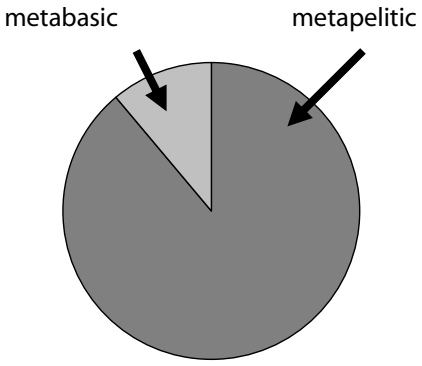

6406/2-1, 4429.85 m
Garn Formation (sand type MN4)

N = 54

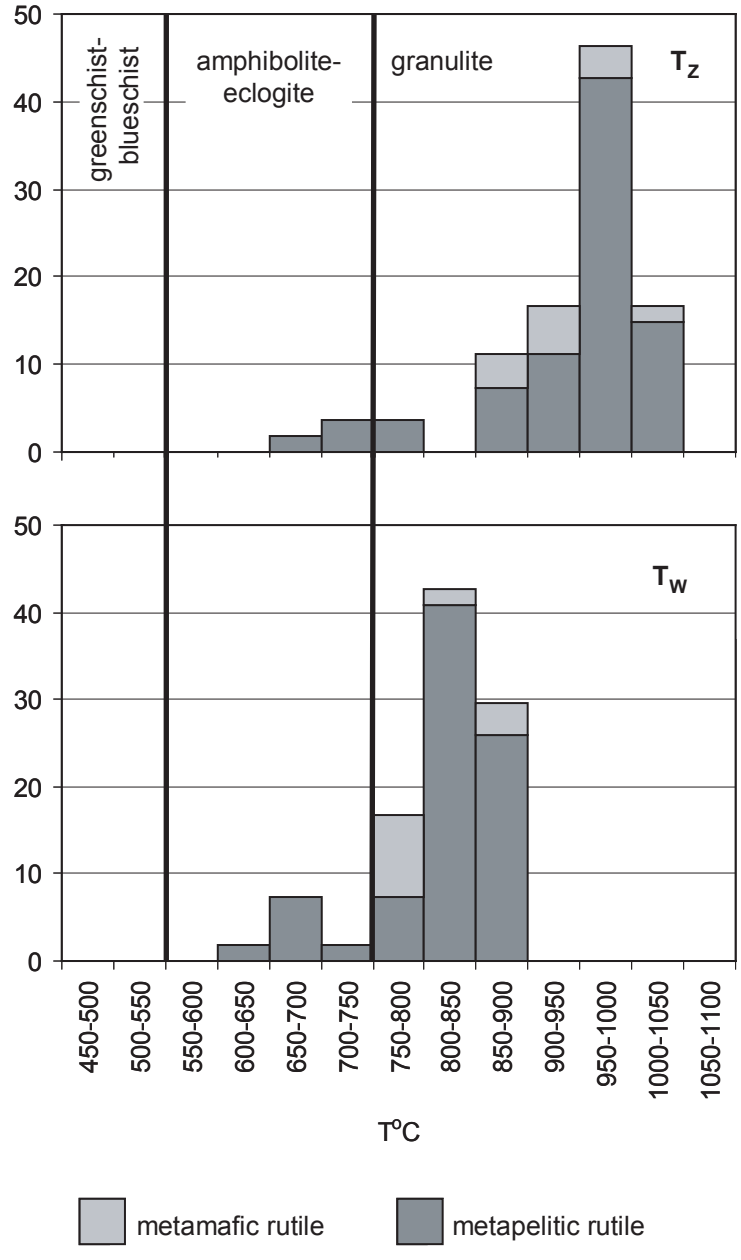
50
40
30
20
10
0
greenschist-
blueschist
amphibolite-
eclogite
granulite
T_Z
50
40
30
20
10
0
T_W
450-500
500-550
550-600
600-650
650-700
700-750
750-800
800-850
850-900
900-950
950-1000
1000-1050
1050-1100
T°C
metamafic rutile
metapelitic rutile

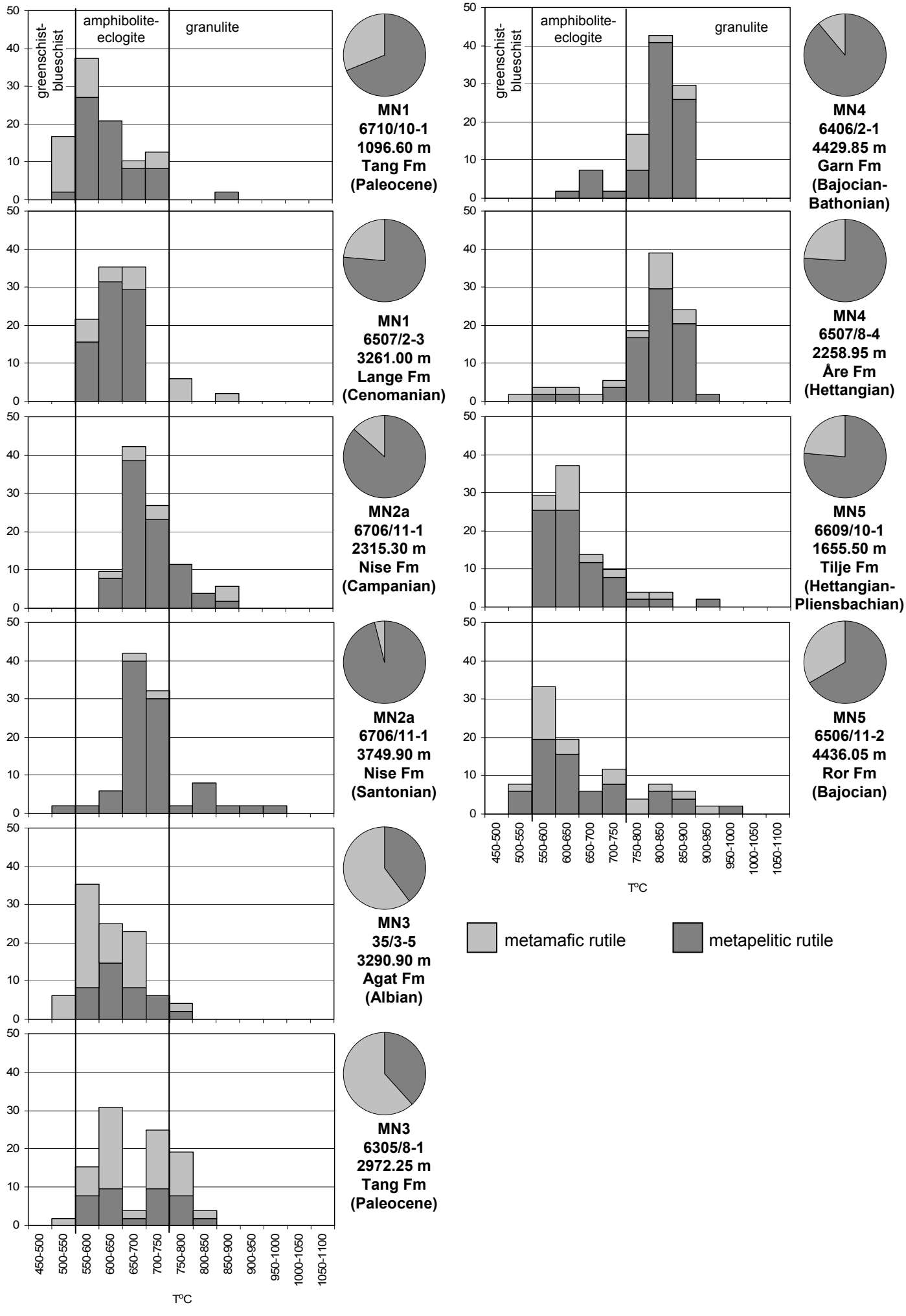
greenschist-blueschist
amphibolite-eclogite
granulite
MN1
6710/10-1
1096.60 m
Tang Fm
(Paleocene)
MN1
6507/2-3
3261.00 m
Lange Fm
(Cenomanian)
MN2a
6706/11-1
2315.30 m
Nise Fm
(Campanian)
MN2a
6706/11-1
3749.90 m
Nise Fm
(Santonian)
MN3
35/3-5
3290.90 m
Agat Fm
(Albian)
MN3
6305/8-1
2972.25 m
Tang Fm
(Paleocene)
MN4
6406/2-1
4429.85 m
Garn Fm
(Bajocian-Bathonian)
MN4
6507/8-4
2258.95 m
Åre Fm
(Hettangian)
MN5
6609/10-1
1655.50 m
Tilje Fm
(Hettangian-Pliensbachian)
MN5
6506/11-2
4436.05 m
Ror Fm
(Bajocian)
450-500
500-550
550-600
600-650
650-700
700-750
750-800
800-850
850-900
900-950
950-1000
1000-1050
1050-1100
TºC
metamafic rutile
metapelitic rutile